Indirect Adaptive Control of a Cyber-Physical Solid-Oxide Fuel Cell Hybrid Energy System

by

Mychal Amoafo

Bachelor's of Science Engineering Science, University of Pittsburgh, 2023

Submitted to the Graduate Faculty of

the Swanson School of Engineering in partial fulfillment

of the requirements for the degree of

Bachelor's of Philosophy

University of Pittsburgh

2023

UNIVERSITY OF PITTSBURGH

DEPARTMENT OF MECHANICAL ENGINEERING AND MATERIAL SCIENCE

This thesis was presented

by

Mychal Amoafo

It was defended on

December 8, 2023

and approved by

Dr. Nikhil Bajaj, Department of Mechanical Engineering and Material Science

Dr. William Clark, Department of Mechanical Engineering and Material Science

Dr. Daniel Cole, Department of Mechanical Engineering and Material Science

Dr. David Tucker, United States Department of Energy, National Energy Technology Laboratory

Indirect Adaptive Control of a Cyber-Physical Solid-Oxide Fuel Cell Hybrid Energy System

Mychal Amoafo, B.Phil

University of Pittsburgh, 2023

The ability of a system to maintain its performance despite changes to its environment is known as adaption. This type of behaviour is prevalent in biological systems and is leveraged in control system to achieve optimal performance when the state variables of a parameter changes. Adaptive control systems leverage system identification to update controller parameter to ensure the stability of a system.

The ability to design optimal controllers by identifying changes in system model makes adaptive control attractive for dispatchable energy systems. Dispatchable energy systems are power systems capable of responding rapidly to grid fluctuations by providing or removing power from the grid, enhancing grid resiliency. The solid-oxide fuel cell gas turbine (SOFC-GT) integrates a solid-oxide fuel cell stack with a micro-gas turbine. It can operate as an dispatchable energy system. Due to highly coupled nature of the SOFC-GT system, the dynamics are inherently nonlinear, and control with linear controller produces sub-optimal control. Ensuring that SOFC-GT systems can undergo rapid-load transitions requires the use of advances algorithms that can control critical process parameters like turbine speed, mass-flows, pressures, temperature gradients across the SOFC stack, etc. Dispatchable energy systems must also operate at off-design operating conditions (partial electric loads) where the a controller designed for nominal operating conditions (full electric load) may perform poorly. Adaptive control will allow the updating of controller gains throughout the entire operating envelope of a dispatchable energy asset, capturing changes to a plant parameter due to different system configures by leveraging system identification.

In highly coupled advanced power systems, like any other mechanical system, system components degrade. For example, in a SOFC-GT system, the recuperator, a type of heat exchanger, the insulation may degrade after multiple cycles. The degrading insulation decreases the efficiency of the heat exchanger. In this scenario, to reach a target temperature

requires more heat needs to be provided to the heat exchanger, more fuel needs to be burned compared. The promise of adaptive control is to account for this change in the system and designed an optimal control law that reduces the required fuel to reach the target temperature.

This paper investigates the indirect adaptive control, specifically adaptive pole placement control, where system identification and controller design are performed to ensure safe operating conditions. This work implements recursive system identification and pole placement for control design. The complete adaptive pole placement control is not implemented, the updating controller coefficients are not used in the feedback loop. Although, the updated controller is not in the feedback loop, insights about adaptive pole placement control can be surmised from the preliminary results.

The feasibility of adaptive pole placement is discussed in this work. Issues in system identifying and controller design are discussed. Potential solutions to overcome these issues is discussed.

Table of Contents

List of Tables

List of Figures

Preface

This thesis is dedicated to my parents

1.0 Introduction

In response to the global push to mitigate the effect of climate change by reducing greenhouse gas emissions, renewable power generation assets such as wind and solar are becoming more commonplace to decarbonize the electric grid. These technologies are being integrated with thermal power plants like combined cycle natural gas, coal-fired, and nuclear power plants. Thermal power plants typically operate as base load power sources, producing a consistent amount of electricity over a given time period [1]. Unlike their thermal counterparts, wind and solar are intermittent, producing irregular amounts of power due to changes in environmental conditions such as temperature, cloud coverage, wind velocity, etc. The interaction between the intermittent and base load power generation assets leads to issues balancing supply and demand of electricity [2]. During the midday hours, there is power overgeneration due to multiple competing power generation assets: conventional power plants and renewable power generation assets. Power supply exceeds demand, negative electricity prices arise. Conventional power plants must sell electricity at negative prices or shut down production. Losses incurred from selling at these prices do not exceed those incurred from shutting down operations [3].

Resolving this issue has motivated the development of dispatchable power generation assets, power plants capable of flexible operation, responding to grid fluctuations by rapidly ramping up or down [2]. Dispatchable power plants, especially one integrated with micro gas turbines has emerged as a competitive technology to enable flexible operation of thermal power plants due to their high fuel flexibility, minimal maintenance, reduced environmental impact, and small footprint [4]. Dispatchable energy systems, such as the solid-oxide fuel cell gas turbine systems (a hybrid cycle with an integrated micro gas turbine and solid oxide fuel cell stack), are seen by the United States Department of Energy (US DOE) as a promising technology to meet their objective of developing power generation technology with higher electrical efficiency, minimized environmental pollution, electricity generation at competitive prices, and sequestering and storing of carbon dioxide [5].

1.1 Solid-Oxide Fuel Cell Gas Turbine Systems

A solid-oxide fuel cell gas turbine is a hybrid or integrated energy system where multiple energy storage and/or generation devices are present in a power generation cycle [6]. Solid oxide fuel cells (SOFC) are electrochemical devices that convert chemical energy in fuels into electricity using electrochemical reactions [5] [7]. Compared to other fuel cell technology, they operate at relatively high temperatures, enabling the use of a various hydrocarbons. Another advantage of their ability to operate in high temperature environments is their use in co-generation, increasing a systems efficiency [5][7]. SOFC power plants have been used extensively in residential, commercial, and industrial applications. It is obvious that the standalone SOFC power plants are attractive alternative energy technology [5]. In power generation, the SOFC is an attractive technology because it can be integrated into a wide range power plants and the exothermic reaction can be used for co-generation as well as drive bottomed thermodynamic cycle [7] like the solid oxide fuel cell gas turbine (SOFC-GT) [5].

The emergence of the solid oxide fuel cell gas turbine (SOFC-GT) hybrid system was motivated by the need of the gas turbine industry to reduce their greenhouse gas emissions. The integrated fuel cell and gas turbine potentially operate at higher efficiencies than their standalone configurations [8]. It has been shown that these systems can reach net electrical and global efficiencies close to 70% and 85%, respectively []. The SOFC-GT hybrid system has been identified by the United States Department of Energy (US DOE) as a promising technology to meet their objective of developing power generation technology with higher electrical efficiency, minimized environmental pollution, electricity generation at competitive prices, and sequestering and storing of carbon dioxide.

Dynamic simulation has indicted that SOFC-GT systems can undergo rapid load transitions; however, demonstrations with physical hardware is limited [8]. There are several experimental facilities researching SOFC-GT systems, the Hybrid Performance facility built by the National Energy Technology Laboratory (NETL) of the US DOE is one such facility. It uses a hardware-in-the loop approach, where a real-time model of SOFC is integrated with a physical cycle containing a gas turbine to test and validate control strategies [8]. Control of the hybrid energy systems during dynamic load changes is difficult due to the coupling of multiple system components. Beyond the SOFC and GT, systems components can include recuperators, reformers, bypass valves, and other power generation equipment [8].

The highly coupled nature of hybrid energy systems such as the SOFC-GT combined with the need to operate at off-design conditions presents a difficult control problem because system stability and operating efficiency must be maintained at partial load conditions. Non-dispatchable power generation systems use the conventional proportional-integral-derivative controller due to their ease of implementation. Degradation of the controller performance is not an issue because these systems operate at their predetermined design conditions and are not expected to operate at other load conditions.

In transient operation where nonlinear dynamics are present, the stability of the controller degrades [4]. Advanced controllers are required to control the highly nonlinear, time variant and large time delays process [4]. At off-design conditions and transient operations, the system dynamics are highly non-linear, the PID controller, optimized for linear dynamics, is not well suited. Performance degradation does not necessarily mean that the system is uncontrollable; it can also lead to a reduction in overall operating efficiency. The thermal coupling of the SOFC-GT cycles nearly doubles the efficiency of coal-fired power plants used in large scale power product; however, this coupling produces highly nonlinear dynamics that require advanced controllers [4, 9].

Previous work the research group at the Hybrid Performance facility located at the National Energy Technology Laboratory in Morgantown, WV indicates that adaptive control is required to cope with degrading performance of controller to maintain performance targets. Key to this endeavor is development of an online parameter estimation to characterize drift from optimal performance. The online estimation algorithm is coupled with real time updating of a controller to maintain stable performance over a broad range of operating conditions.

System identification is a method of developing mathematical descriptions of a system by observing the inputs and outputs of a real process. System identification is a vital tool in real time updating of controllers to ensure optimal performance because it tracks how the parameters of a model changes due to changes in the operating environment like the introduction of disturbances. In the SOFC-GT system, electric load is treated as a disturbance.

The novelty of this work is the investigation of closed-loop system identification, a deviation from most system identification methods which rely on open-loop data attained from bump or step tests, where the input is varying to produce a system response. Here we aim to identify the process function from the closed-loop process by considering the outputs of the controller and the output of the process. Closed-loop identification will enable improved offline system identification and controller development because the system can undergo more rigorous testing that is not feasible when there no controller in the feedback loop due to safety concerns and risk to equipment. Closed-loop identification will also enable the adaptive control, if a suitable model for control is identified from the data, linear control design techniques can be readily used to produce a robust controller. The controller parameters can be improved during operation.

The objective of this work is to demonstrate the feasibility system identification algorithms (open-loop and closed-loop) for model development. It will cover experimental design, recursive estimation algorithms, pole placement control, and adaptive pole placement control.

1.2 Adaptive Control

Adaptation is the ability of a system to maintain its performance despite changes to the environment containing the system. The same principles hold in control systems where adaptation refers to the ability of a system to maintain its performance targets when the system undergoes large changes to itself (changes in state variables) or its environment [10]. The goal adaptive control is the real-time control of dynamic system with uncertainty using adaptation and system identification [11]. Adaptive control emerged from the aerospace industry where autopilot systems where being designed for flight control applications. The objective was to deal with the wide range of operating conditions experienced by high-performance aircraft by developing regulators that could adapt in real time, changing the controller gains to expand the flight operating envelope. Several advances were made in adaptive control in the early 1950s for flight control systems incorporating aerodynamics, guidance, navigation, and control, and adaptation [10, 11]. Since the initial breakthrough up till now, the field has received enormous research interest, from developing analytical tools to ensure stability to the incorporation of neural networks. The following provided frameworks for stability and robustness. A brief history and overview of adaptive control is provided in [10] and [11].

Popular adaptive control methods include: Model Reference Adaptive Control (MRAC), Adaptive Pole Placement Control (APPC), Adaptive Sliding Mode Control (ASMC), and Extremum Seeking (ES) [10]. These methods can be broadly categorized into three categories open-loop adaptive control, model-reference adaptive control, and indirect adaptive control [10]. The following subsections briefly discuss the three main approaches.

1.2.1 Gain Scheduling

Open-loop adaptive control, also known as gain scheduling, is a control strategy where gains are adjusted correlating auxiliary variables to process dynamics. [12]. The approach is illustrated in the Figure 1. They key assumption underlying the gain scheduling approach is the a strong relationship between measurable values in the environment and the plant [13]. An example of gain scheduling can be found in flight control where sensors measuring pressure is used to update controller gains, because changes in pressure may indicate a new operating condition. Gain scheduling does not used feedback from the process. The efficacy of this approach is diminished when the relationship between a measurable variable in the environment and the plant changes [13].

1.2.2 Model Reference Adaptive Control

Model Reference Adaptive Control (MRAC) has a long history in adaptive control. It was developed to improve performance across the flight envelopes of flight control systems [10]. MRAC is an adaptive control structure where the desired performance of a minimum phase system is represented by a model that produced a desired response to a command Signal. The block diagram for a MRAC is shown in Figure 2. The command or reference

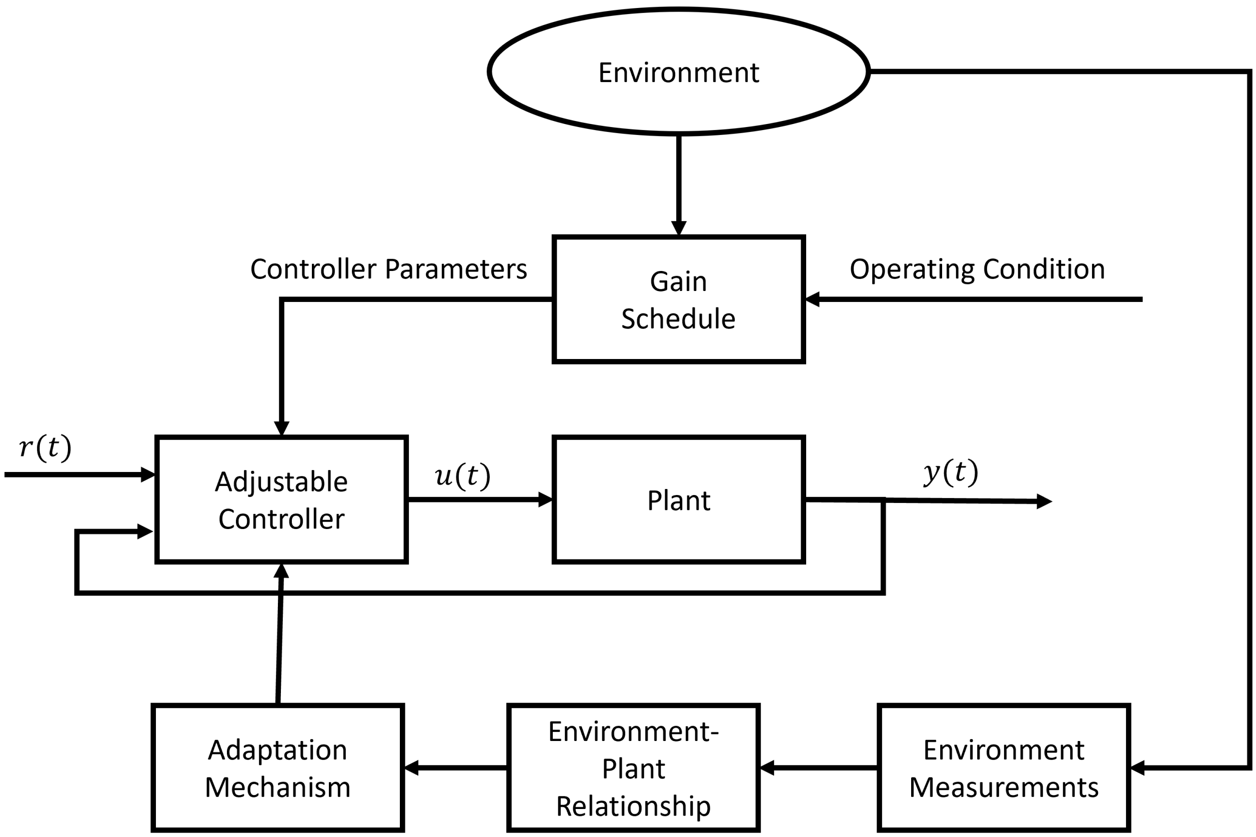

Figure 1: Block Diagram of Gain Scheduling

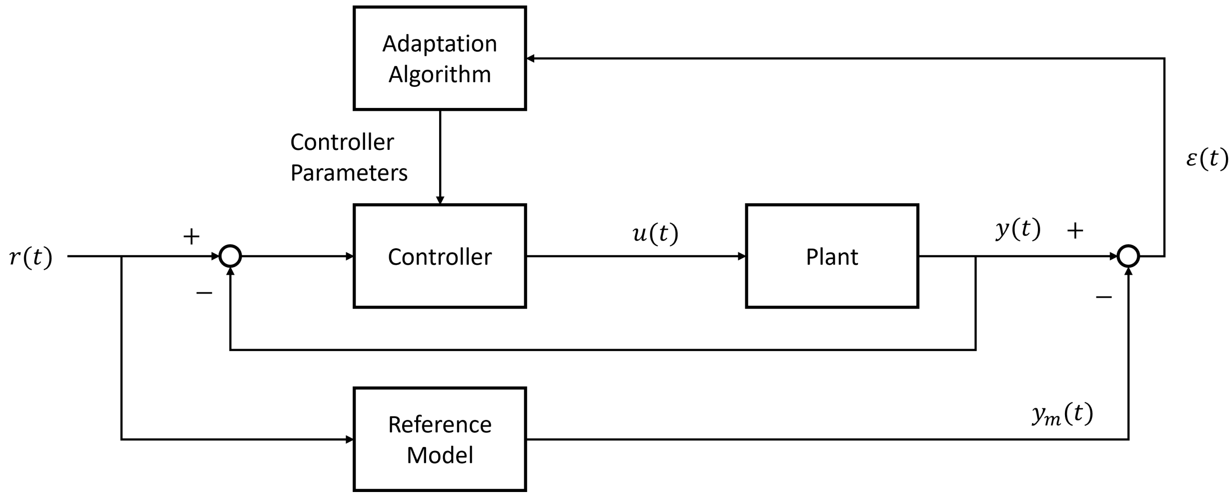

Figure 2: Block Diagram of Model Reference Adaptive Control

signal is sent to both the reference model and the actual system, the error between the actual system and the reference model drives an adaptation algorithm that adapts the gains of the controller to minimize the error between the actual system and the reference model [10][13].

1.2.3 Adaptive Pole-Placement Control

Adaptive Pole Placement Control (APPC) is the largest class of adaptive control methods because it is extendable to systems with minimum and non-minimum phase behaviour. The APPC is a self-tuning regulator (STR), where the parameters of the plant are estimated using a recursive estimation method. The estimated parameters are then used to design a controller. The control design strategies include pole placement, minimum variance, linear quadratic, etc. [12]. The recursive estimation algorithm can include stochastic approximations, least squares, extended, and generalized least squares, maximum likelihood, and instrument variable. The choice of estimation algorithm depends on the model structure. For example, an extended least squares algorithm is used for parameter estimation of a auto regressive moving average with exogenous inputs (ARMAX). Figure 3 illustrates the APPC approach. APPC works by identifying a plant model using the input and output of the plant

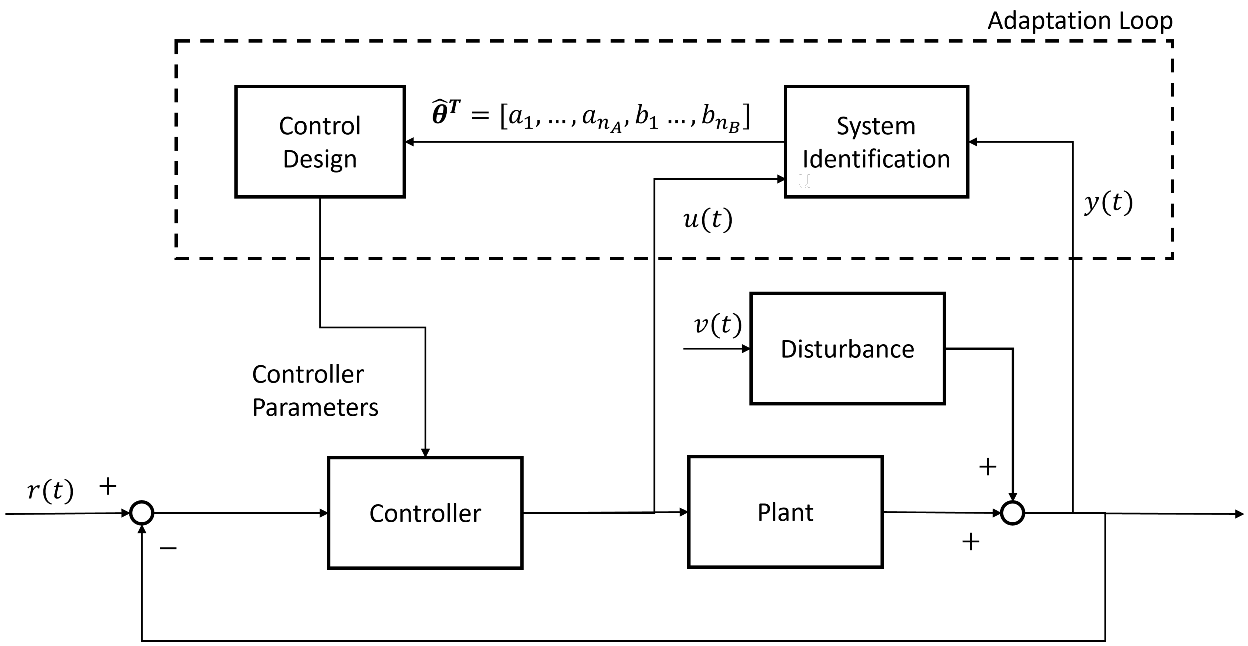

Figure 3: Block Diagram of Adaptive Pole Placement Control (APPC)

model of interest. After parameter estimates are identified, they are used to design a digital controller. To solve the pole-placement problem, the desired closed-loop algorithm defined by the user and is used to solve a system of linear equations.

1.2.3.1 Pole-Placement Design: Polynomial Approach

The control design procedure begins with a process model. The model can be derived using first principles or experimental data. The plant can be described by the following difference equation for a single input, single output system.

$$A(z)y(t) = z^{-d}B(z)u(t) + A(z)v(t) \tag{1}$$

Once a model has be derived or identified, a two degree of freedom controller is designed. The controller is designed for a linear system with output feedback. The controller being designed in this study has one output, the control action, and two inputs: the reference or

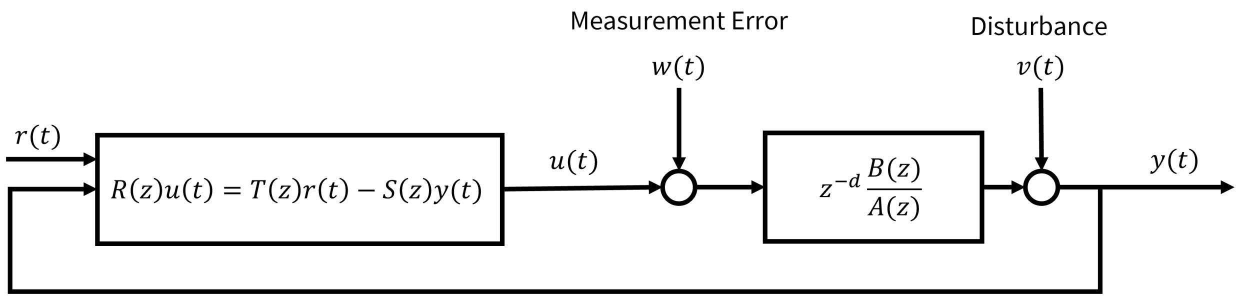

Figure 4: Control Loop with an RST Controller

command signal and the process output. The two degree of freedom controller is represented by

$$R(z)u(t) = T(z)r(t) - S(z)y(t) \tag{2}$$

The controller consists of the polynomials $S(z)$, $R(z)$, and $T(z)$. The R and S may be selected to achieve certain characteristics: proportional control, integral action to ensure zero-steady state error, etc [13][14]. The T polynomial may be selected for tracking dynamics [14]. It is also possible to select R and S polynomials to operate as filters, where they defined to achieve a some desired performance. Beyond filtering, the polynomials can be selected to achieve zero steady state error for a step disturbance.

Solving the control design process begins by finding the equation of a closed-loop system. From Figure 4, the closed-loop system is defined by

$$(A(z)R(z) + B(z)S(z))y(t) = B(z)T(z)r(t) \tag{3}$$

The characteristic equation of the closed-loop system is

$$A_{cl} = A(z)R(z) + B(z)S(z) \tag{4}$$

Pole-placement design can be reduced to an algebraic problem where the objective is to find the polynomials $R(z)$ and $S(z)$ given the polynomials $A(z)$, $B(z)$, and $A_{cl}(z)$. In the APPC, the polynomials $A(z)$ and $B(z)$ are identified from process measurements at each sampling period. The polynomial $A_{cl}(z)$ is defined by the used to achieve a desired transient response. Equation 5 is known as the *Diophantine equation*. Solving the *Diophantine equation* involves specifying the degrees of the polynomials to ensure uniqueness of a solution, causality of the controller, or to achieve a minimum degree solution.

The polynomial $A_{cl}(z)$ can be factored as

$$A_{cl}(z) = A_c(z)A_o(z) \tag{5}$$

where $A_c(z)$ corresponds to the controller polynomial. This polynomial is contains the poles of the desired response. $A_o(z)$ is the observer polynomial. A thorough explanation of the derivation of the observer polynomial is provided in [14].

After selecting the $A_{cl}(z)$ and solving for the $R(z)$ and $S(z)$ polynomial, the polynomial $T(z)$ is selected to achieve a desired response to a change in the reference or command signal. The selection of $T(z)$ polynomial depends on the zeros of the process model and the possible values of polynomial $T(z)$ are discussed in [14]. Pole placement is only valid when the following assumptions hold [13]:

1. No restriction upon the orders of the polynomials and the delay d.
2. The order of the polynomials and the coefficients of the plant model are known.
3. The zeros of the can be within or outside the unit circle.
4. The polynomials $A(z)$ and $B(z)$ do not have any common factors.
5. The zeros of $A(z)$ can be inside or outside the unit circle.

Solving the *Diophantine equation* can be done using matrix calculations when the degrees of the polynomials are known. In this study, the degrees of the polynomials are selected to ensure a causal controller. Integral action is incorporated in the controller,ensuring zeros steady state error, by selecting the degree and factors of $R(z)$. The matrix form of the *Diophantine equation* is

$$
\begin{bmatrix}
a_0 & 0 & \cdots & 0 & 0 & \cdots & \cdots & 0 \\
a_1 & 1 & \ddots & \vdots & b'_1 & 0 & \ddots & \vdots \\
\vdots & & \ddots & 0 & \vdots & & \ddots & \\
 & & & 1 & & & & 0 \\
\vdots & & & a'_1 & \vdots & & & b'_1 \\
a'_{n_{A'}} & & & & b'_{n_{B'}} & & & \\
0 & \ddots & & \vdots & 0 & \ddots & & \vdots \\
\vdots & \ddots & & & \vdots & \ddots & & \\
0 & \cdots & 0 & a'_{n_{A'}} & 0 & \cdots & 0 & b'_{n_{B'}}
\end{bmatrix}
\begin{Bmatrix} r_0 \\ \vdots \\ r_{n-1} \\ s_0 \\ \vdots \\ s_{n-1} \end{Bmatrix}
=
\begin{Bmatrix} \alpha_0 \\ \alpha_1 \\ \vdots \\ \alpha_n \\ \alpha_{n+1} \\ \alpha_{n+2} \\ \alpha_{2n-1} \end{Bmatrix} \quad (6)
$$

The matrix on the left is known as the *Sylvester matrix.* It can be seen readily from the matrix formulation of the *Diophantine equation* that the order of the polynomials will produce different solutions. Solving this equation in real-time can be done using Gaussian elimination.

1.3 An Overview of Adaptive Control for Hybrid Energy Systems & Thermal Power Plants

The SOFC-GT system was initially developed jointly Siemens and Westinghouse in the 1990s to develop technology to target the distributed generation market that was emerging in the late 1990s [15]. The initial hybrid technology featured a tubular SOFC that was pressurized and integrated with a gas turbine, producing a system with efficiencies of 70-75%.

Despite the optimism initially expressed by Westinghouse to target the technology for the distributed generation market, commercialization was failure to control of the hybrid energy system proved difficult. Research to develop adaptive controller that can enable operation of the SOFC-GT hybrid energy system a wide range of conditions is still ongoing. This section will provide an overview of adaptive controllers to control of SOFC-GT system.

Juardo et al. [16] presented an adaptive minimum variance control for a molten-carbon fuel cell (MCFC) and microturbine hybrid power plant. The paper focuses on controlling stack current. The plant in this system is generated from first principles and is simulation using MATLAB. The system that is model consists of a250 kW fuel cell state with a 30 kW gas turbine, a heat recovery unit, power conditioning system (inverter), and controller. The inverter is assumed to perfectly control the voltage and has an inversely proportional relationship to stack voltage. The dynamics of the inverter are not considered. The model is used to investigate the transient behaviour of the SOFC-GT systems, this is achieved by assuming the plant operates at steady state conditions at the rated power. The electric load demand of the system is varied. To achieve minimum variance control, a model must be identified. The plant model is assumed to be a discrete linear stochastic model. Stochastic model allow the inclusion of the impact of disturbances on the plant output, load changes are treated as disturbances in the system. The load power variation is zero mean, white noise with a constant variance σ^2. A recursive least squares algorithm was used for estimate parameters for the stochastic model. A minimum variance control control algorithm was used. The performance of the controller was demonstrated by varying the operating conditions. To demonstrate the robustness of the controller, the gas concentration was changed during the simulation. The minimum variance controller proposed by Juardo et el. [16] demonstrated promising results

Tsai et al. proposed MRAC structure for controlling an SOFC-GT system. This study used system identification to identify a plant model from experimental data. The authors develop transfer functions describing the relationship between mass flows caused by changes in the fuel valve and cold-air bypass valves and transfer functions for the relationship between the turbine speed and the fuel valve and cold-air bypass valves. The identified models were used to replicate the key dynamics of interest. After identifying the model, a model reference adaptive controller was developed. The authors compared the results of the MRAC to a proportional integral (PI) controller. The authors tested in the controllers in various conditions. They found that the MRAC performed considerably better than PI controller when reference signal undergoes step changes. The PI controller exhibited a 600 rpm overshoot on average and was unable to maintain the nominal speed of 40500 rpm. The MRAC initially has a slow response as the adaptation measure need to converge. During the first 200 seconds of the tests the PI and MRAC controller are not equivalent because the MRAC controller has a slow initial response as the parameters converge. The authors also generate a second set of reference signal step changes to force the system beyond the linear range. In this instance the MRAC controller was able to handle the force nonlinear behaviour. As expected, the PI controller did not fare will in this scenario. The authors concluded that the benefit of the MRAC was the ability to deal with nonlinear behaviour very simply and meeting transient specifications in a safe manner. The discussion section of the paper is quite fruitful as the authors highlight how best to integrate a MRAC into a hybrid energy system. They consider extending its use to regulate the other actuators in the system and provide insight into the best possible candidates.

2.0 Methodology

2.1 The Hybrid Performance Project

Built in 2002, the Hybrid Performance (Hyper) facility, is a novel test bed for advancing hybrid power generations systems. [6]. The Hyper facility uses an innovative hardware-in-the loop approach where a software components are coupled with hardware components to replicate the behaviour of a fully functional SOFC-GT system [17]. The facility main components are system are a micro gas turbine and a solid oxide fuel; the micro gas turbine is a physical component and the SOFC exists as a computational model. The two components are coupled through a series of middle ware, sensors, and actuators. This approach enables rapid testing and developing of technologies that can be integrated into the cycle and is extendable to other hybrid cycles involving a gas turbine [17]. For example, the performance of a nuclear gas turbine hybrid can be replicated by changing integrating a computational nuclear model. This occupies a space between a fully computational model of a power system and pilot plant, it enables simultaneous controls development and system integration. It reduces the risk associated with evaluating dynamic control strategies necessary to meet flexibility requirements of grid tied SOFC-GT systems. It does not entirely mitigate risk as surge and stall can still occur; however, the SOFC model can be easily restarted if a controller fails to regulate the temperature gradient across the fuel cell stack. This ensures the technological development of the SOFC-GT system is not cost prohibitive. elevating research in the field from physics based models to a hardware-in-the loop approach where control strategies must be sufficiently advanced to ensure multi-objective control and straightforward to implement on an industrial controller.

Beyond the applications to developing a SOFC-GT cycle, the CP approach represents a new paradigm for energy technology development by addressing the technology death valley, overcoming the "one-shot" mentality common in energy and power generation industry [18]. Energy technology development starts with laboratory experiments, numerical simulations, and building a pilot plant to understand the feasibility of the technology before large scale plant production [18]. The “one-shot” mindset is a product of this approach where failure at the pilot scale impedes the commercialization of the technology due to skepticism from investors. If the energy technology is still pursued after failure at the pilot plant stage, development recommences at the laboratory scale [18]. The hardware-in-the-loop systems represent an opportunity to radically change the energy technology development process by combining hardware and numerical models, introducing an opportunity to iteratively design power generation systems, reducing risk of failure at the pilot and cost of development [18]. It occupies the gap between laboratory scale models and the pilot plant stage, providing a relatively inexpensive approach to thoroughly evaluate the technology and discover potential hurdles that may impede commercialization.

The Hyper facility replicates the performance of 300 kW SOFC-GT hybrid energy generation system. Figure 5 shows the physical components of test facility. The system features a 120 kW Garret Series 85 Auxiliary Power Unite operating at a nominal rotational speed of 40,500 rpm and a pressure ratio of four. It is coupled to a gear driven synchronous (400 Hz) generator. The airflow from the exhaust and the discharge of the a two-stage radial compressor are routed to two Solar Turbine counter flow primary surface recuperators to preheat the air going to the SOFC stack. A plenum replicates the pressure drop across a physical SOFC stack. A natural gas burner is used to simulate the exhaust of the SOFC stack, completing the thermal integration of the system. The facility includes three bypass valves used to control airflow throughout the system. The hot air (HA) bypass valve controls the cathode inlet temperature (air going into the plenum). The bleed air (BA) bypass valves is used to. The cold air (CA) bypass valve controls. Electrical load is dissipated using an resistive load bank. The facility is equipped a suite of instrumentation for accurate measurements of gas flows, optical turbine speed, high speed pressure, vibration, and acoustics, and a Raman Gas Analyse for gas composition [9].

Monitoring and controls of process parameters are conducted using a Woodward Micronet computer with a five millisecond sampling frequency. A Bently Nevada Adre system is used for acoustic data processing. The fuel cell model is a 1-dimensional numeric model, converging within five milliseconds. The model controls the fuel cell model when the SOFC stack is used to simulate the entire SOFC-GT (the system can be operated without the model controlling the fuel valve, producing a recuperated gas turbine cycle). The model connected with the plenum can replicate the physical behaviour of a “real” fuel cell stack [9].

2.2 Experimental Design

The development of a model-based controller begins with system identification, derivation of a mathematical model from observed input and outputs. In this work, the objective is to produce a discrete transfer function describing the relationship between the fuel valve and the turbine speed. To generate models for control, experiments are designed to produce data sets that enable system identification. Identification can occur either in open-loop (no controller in the feedback look) or closed-loop (controller in the feedback loop). These experiments are step or relay feedback tests. Step tests are usually performed in open-loop, but is readily applied to closed-loop identification. The benefit of open-loop identification is the direct correlation between inputs and outputs. In closed-loop, this correlation is less straightforward. Although open-loop tests are straightforward, many systems unstable in open-loop and identification must be completed with a controller in the feedback loop to ensure stability. The specifics of closed loop identification are covered in the following chapter.

2.2.1 Open-Loop Step Tests

In the open-loop tests the Hyper facility is fixed around an operating condition determined by a combination of electric load bank, cold-air, hot-air, and bleed air bypass valve. The turbine speed fuel valve controller is fixed at user-defined value and the fuel valve undergoes step change. This ensures that the relationship between the fuel valve and the turbine speed is easily understood.

To begin the open-loop step test, the electric load, cold-air, hot-air, bleed air bypass valves positions are fixed around the desired operating condition. After changing the aforementioned inputs, the Hyper is brought to a steady state condition. Steady-state is deter-

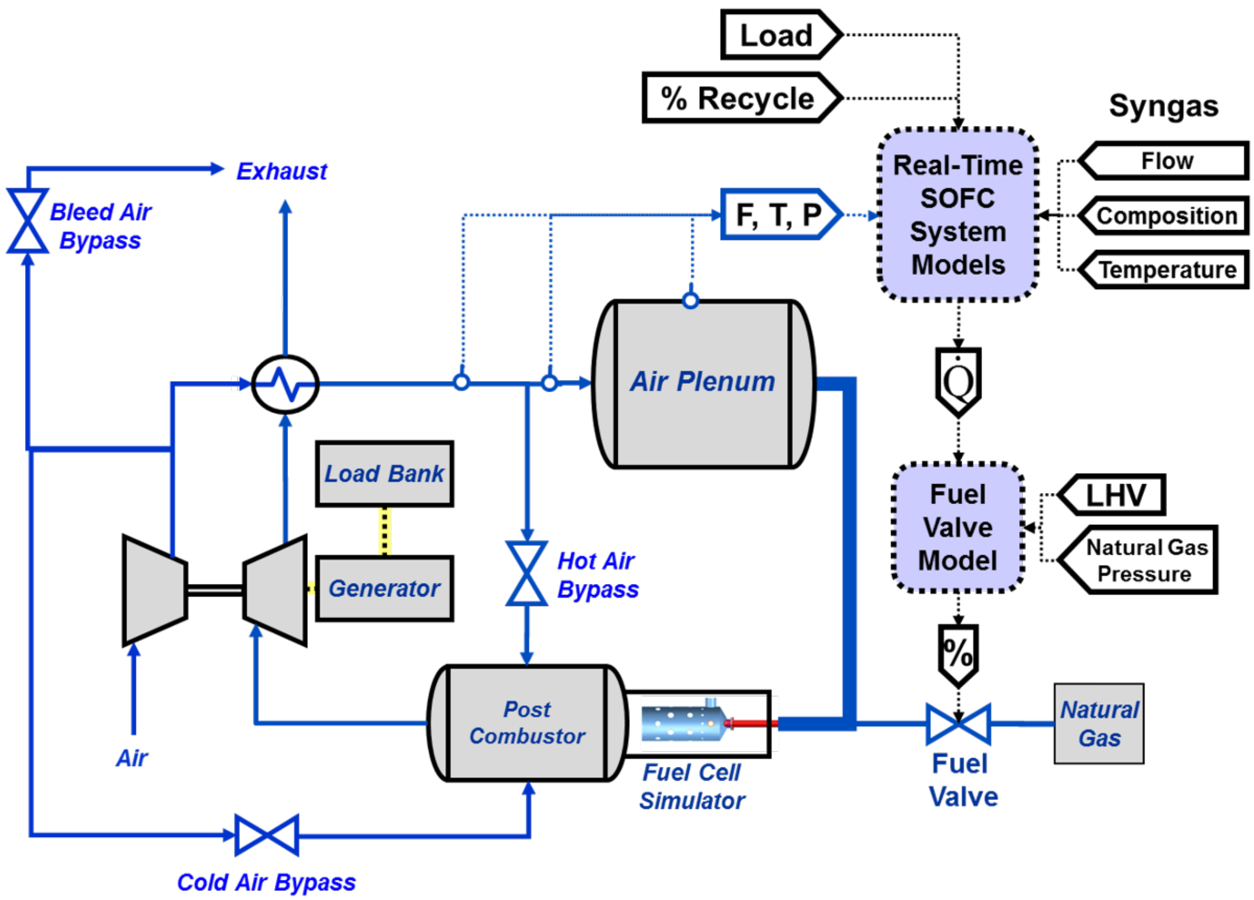

Figure 5: Diagram of the SOFC-GT at the Hybrid Performance Facility

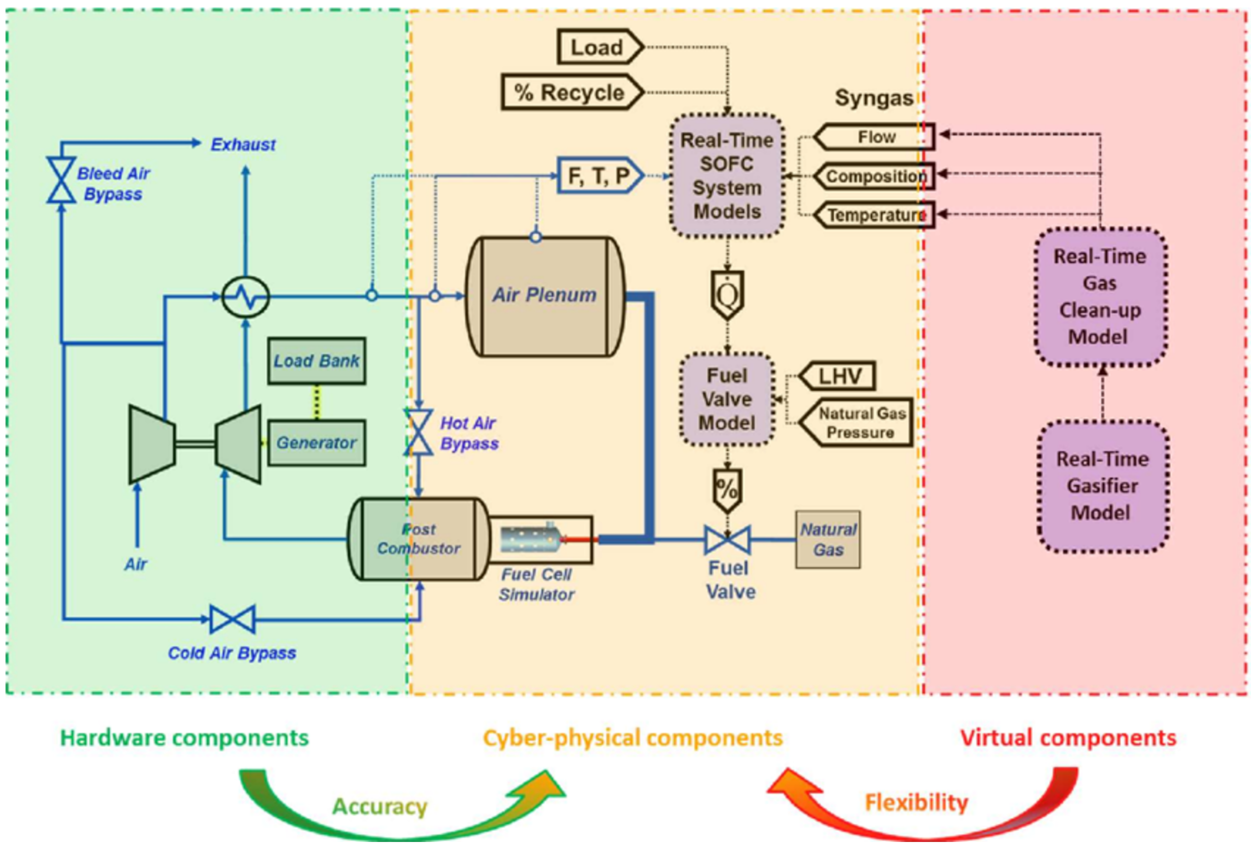

Figure 6: Hardware, Middle, and Hardware in the Hybrid Performance Facility

mined by the change in the skin temperature of the plenum over a fifteen minute period. After the steady state condition is reached, the turbine speed fuel valve position is fixed, putting the Hyper in open-loop. The fuel valve is varied by two percent from the nominal fuel valve position. This test is typically repeated at multiple operating conditions to explore how the turbine speed and fuel valve transfer function changes with respect to changing operating conditions change.

2.2.2 Closed-Loop Step Tests

The closed-loop step tests are similar in approach to the open-loop step tests; however, the objective of this tests is to generate data that will enable the modeling of the relationship between the fuel valve and turbine speed when a disturbance is introduced to the system. In this study, the electric is treated as a disturbance.

The test begins with fixing the electric load and the bypass valves around the desired operating conditions. The Hyper is brought to its steady-state condition. The turbine speed fuel valve is in the feedback loop, it is not fixed at a single position, ensuring the turbine speed is maintained. The turbine speed set point in the Hyper is 40,500 rpm. The electric load is varied by 5 kW around a predetermined value.

Closed-loop identification is not straightforward, it is the subject of extensive research; however, it is critically important in adaptive controls, especially self-regulating controllers, where identification and control occur simultaneously. Although, online closed-loop system identification is not tested in the experimental facility, the offline closed-loop identification provides insight into the viability of various algorithms for identification without the need for multiple experiments. In a complex system like the Hyper with many inputs, closed-loop identification enables the exploration of how changes in the inputs impact the relationship between the fuel valve and turbine speed.

2.3 MATLAB & Simulink

The studies discussed in the Results section rely on MATLAB and Simulink. This study relies on open-loop and closed-loop step change tests to develop discrete transfer function to model various processes in the Hyper.

To develop models from the system identification, ARMAX models are considered. The open-loop models have an deterministic ARX structure. A stochastic ARMA model is used for the closed-loop data because the electric load changes are treated as a disturbance and not an input. This enables the uses of single input, single output mode. Recursive least squares and recursive extended least squares are used for deterministic and stochastic parameter estimation, respectively. A sampling period of 5 ms was used.

The system identification process begins with data normalization using the mean and standard deviation of the data [19]. The equation for normalization is given as follows:

$$\bar{x_i} = \frac{(x_i - \mu)}{\sigma} \tag{7}$$

where $\bar{x}$ is the normalized value, μ is the mean, and σ is the standard deviation.

After normalization, the data is split into training and validation data. The input parameters of the recursive least squares algorithm are the order of the numerator and denominator polynomials, the forgetting factor, and the initial gain matrix. The input parameters for recursive extended least squares algorithm are: order of the numerator,denominator, and moving average polynomials, the forgetting factor, and the initial gain matrix. To validate the models the predicted outputs to a given input signal is calculated using the `lsim` function in MATLAB. The auto-correlation and the distribution of residuals are calculate to ensure unbiased parameter estimates. The plotting the distributions of residuals is done by using the `hist` function in MATLAB.

Simulink is used to develop simulations of processes of interest in the Hyper facility.

3.0 System Identification

System identification is the derivation of mathematical models of process models from observed inputs and outputs in a system [19]. Although it has long been the domain of statisticians, system identification emerged as a tool for control engineers in the 1960s [20]. Prior to system identification, engineers developed first-principle models and used the classical feedback control approaches (Bode, Nyquist, Ziegler-Nichols plots) to develop controllers. It was the advent of state-space models in 1960 accompanies by developments in optimal controls and filtering within a linear quadratic framework that motivated advancements in model based control design methods. The advancements in system-identification applied to control theory was motivated a desire to extend the model-based control design techniques to system where no reliable model could be derived from first principles [20].

Unlike other practitioners of system identification, control theorists recognized that for control, the objective of system identification is not to discover the true system, but the best approximate model within a model set. This lead to characterization of model based on the bias and variance of the error of an estimated transfer function. An exact model of a system, it is optimal for all application; however, the quality of an approximate model is dependent ton its intended application. Thus, the purpose of system identification in the controls context is to find the best approximate model with a distribution of error that produces the best controller. This is known as *goal-oriented identification* or *identification for control* and it treats system identification as a design problem. An exhaustive detailing of the history of system identification will not be covered in this work, an excellent treatment of the history of system identification for control is provided by Gevers [20].

Development of a model-based controller begins with developing a model either from first principles or using system identification techniques to achieve a model that best represents the behaviour of the real system. First principles leverages physics to model, system identification is data driven, using mathematics to develop a relationship between inputs and outputs. Most system identification is done offline using a step or feedback relay test.

In these tests, the system is excited. In chemical production plants, where first principle models are not easily derived, system identification is used to develop models for model-based controller like model predictive control (MPC). The objective of system identification in the chemical production context is to produce reduced order that captures the most dominant dynamics of the system. Offline system identification often requires several hours to several weeks of open-loop tests to achieve a model that will produce the best controller.

Although, the Hyper does not require several weeks of open-loop tests to produce approximate model for control. Open-loop tests are impractical because they are time consuming and pose a systemic risk to process equipment. The challenges with open-loop identification has motivated research in closed-loop identification techniques where routine operating data can be used to generate a approximate model for system for model-based control. This makes model development and model-based control designs accessible and attractive because a approximate model can be achieved without increased risk to equipment and saves times. Closed-loop identification methods have been understood for several decades and multiple identification algorithms exist. Closed-loop identification has been an active area of research because of adaptive controller where identification and control occur jointly to deal with complex systems [21].

System identification is classified by a number of approaches: prediction error, subspace approaches, and non parametric methods such as correlation and spectral analysis methods [21]. It is vital in control system for developing models from experimental data when dynamics of the system proves difficult or expensive to model. Generating data for system identification often involves open-loop identification where there is not feedback mechanism ensuring that the input and noise are uncorrelated. It is not always possible to identify a system in open loop. Plants or processes with integrator behaviour or are unstable in open loop are not amenable to open-loop identification and require operation in closed-loop [include citation]. For many industrial plants such as chemical production facilities it is not feasible to operate in open loop due to increased risks to operator safety and equipment damage. In chemical production plants, it is also not economical to operate stop production to operate in open-loop to develop process models for controller development. Such operations require the ability to identify process model from closed-loop operation. The problem with closed-loop identification is that unlike open-loop identification where the input and the noise are uncorrelated to due the feedback being zero, the noise and the input are correlated due the non-zero feedback. Closed-loop system identification techniques are well developed due to the interest of developing model suitable for model-based control design.

Identification of systems under feedback consists of three approaches: direct, indirect, and joint input-output system identification. Direct identification assumes no knowledge of the controller and does not use the reference signal to identify a process model. Indirect identification methods assumes the controller is known and the reference signal is known. The joint input-output approach assumes that the controller is not known; however, the structure of the controller is known [22].

System identification is a vital to the adaptive control approach. The updating of parameter estimates for a process model ensures that the model updates when the dynamics of the physical system, in this case the dynamics between the fuel valve and the gas turbine change. The objective of this work is to provide insight about how the transfer parameter estimates of a transfer function changes as the operating conditions vary. This work considers models from the ARMAX family of discrete transfer functions. This work focuses on direct identification approach for closed-loop identification.

3.1 Deterministic Models

Deterministic models are straightforward, it is assumed that noise does does not impact the system. The deterministic model relationship is given a extensive treatment in [13]. For this work, the deterministic model is only used for open-loop identification. The deterministic model is straightforward and is given by the following equation:

The transfer function for a discrete-time linear process is given below

$$y(t) = z^{-d}\frac{B(z)}{A(z)}u(t) \tag{8}$$

The deterministic model used above is commonly known as the ARX model, it is a part of the larger ARMAX family.

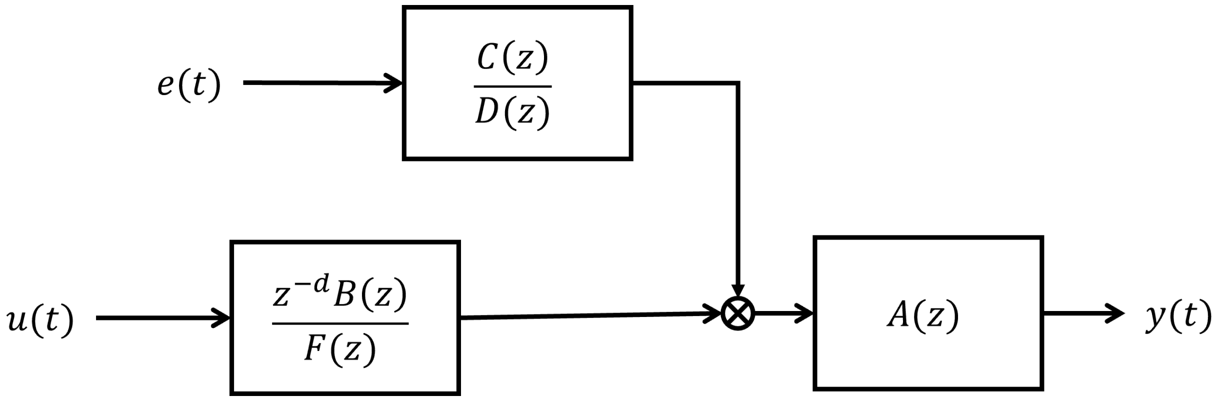

Figure 7: General Polynomial Model

3.2 Stochastic Models

Stochastic refers to randomness, in the context of control, randomness may be due to input disturbances or measurement noise. In system identification, the stochastic model is preferred because it enables the characterization of various disturbances and noise. A general stochastic model for single input, single output (SISO) model is illustrated in Figure 7. This general model, can be simplified by setting the polynomials $B(z)$, $A(z)$ to unity [23]. It can also be extended or augmented for to multiple-input single output (MISO) systems. To find the parameter estimates of the stochastic models recursive extended least squares (RELS) or recursive maximum likelihood algorithms can be used.[23].

The equation for an ARMAX model is given below:

$$y(t) = z^{-d}\frac{B(z)}{A(z)}u(t) + \frac{C(z)}{A(z)}e(t) \tag{9}$$

3.3 Direct Identification for Adaptive Pole Placement Control

Direct identification is the preferred approach of for closed-loop system identification because it works regardless of controller complexity and no knowledge of the controller feedback is required. Well-known algorithms such as recursive least squares can be used in closed-loop identification without modifications. If the noise properties of the process are understood and the model structure is accurate direct identification produces consistent results.

3.3.1 Recursive Least Squares (RLS)

A RLS algorithm is used to for closed-loop identification. The RLS algorithm is described by the equations below.

The vector of measurements is defined below:

$$\phi(t) = (-y(t-1) \ldots - y(t-n_A), u(t-d-1) \ldots u(t-d-n_B))^T \tag{10}$$

where n_B and n_A are the orders of the B and A polynomials of the discrete-time transfer function.

The vector containing the estimated coefficients of the polynomials A and B is defined below:

$$\hat{\theta}(t) = (\hat{a_1} \ldots \hat{a}_{n_A}, \hat{b}_1 \ldots \hat{b}_{n_B}) \tag{11}$$

The derivation of the RLS algorithm is given in [**?**]. The algorithm can simply be described by the following set of equations [23]:

The prediction error $\varepsilon(t)$ is given as follows:

$$\varepsilon(t) = y(t) - \hat{\theta}^T(t-1)\phi(t) \tag{12}$$

The vector of predicted coefficients $\hat{\theta}$ is given as follows:

$$\hat{\theta}(t) = \hat{\theta}(t-1) + L(t)[y(t) - \hat{\theta}^T(t-1)\phi(t)] \tag{13}$$

The updating vector $L(t)$ is given as follows:

$$L(t) = \frac{P(t-1)\phi(t)}{\lambda(t) + \phi^T(t)P(t-1)\phi(t)} \tag{14}$$

The gain matrix $P(t)$ is given as follows:

$$P(t) = \frac{1}{\lambda(t)} \left[P(t-1) \frac{P(t-1)\phi(t)\phi^T(t)P(t-1)}{\lambda(t) + \phi^T(t)P(t-1)\phi(t)} \right] \tag{15}$$

The residual $\bar{\varepsilon}(t)$ is given as follows:

$$\bar{\varepsilon}(t) = y(t) - \phi^T(t)\hat{\theta}(t) \tag{16}$$

The variable forgetting factor $\lambda(t)$ is defined as follows

$$\lambda(t) = \min \left(\lambda_0 \lambda(t-1) + (1-\lambda_0), 1 - \frac{\bar{\varepsilon}^2(t)}{\alpha} \right) \tag{17}$$

where λ_0 and $\alpha > 0$

3.3.2 Recursive Extended Least Squares (RELS)

The RELS differs from the RLS algorithm due to the inclusion of the residual in the vector of measurements. The residual behaves like a moving average, the model used in this study is known as the ARMAX model.

$$\phi(t) = (-y(t-1) \ldots - y(t-n_A), u(t-d-1) \ldots u(t-d-n_B), \bar{\varepsilon}(t-1) \ldots \bar{\varepsilon}(t-n_C))^T \tag{18}$$

where n_B, n_A, and n_C are the orders of the B, A, and C polynomials of the discrete-time transfer function.

The vector containing the estimated coefficients of the polynomials A and B is defined below:

$$\hat{\theta}(t) = (\hat{a}_1 \ldots \hat{a}_{n_A}, \hat{b}_1 \ldots \hat{b}_{n_B}, \hat{c}_1 \ldots \hat{c}_{n_C}) \tag{19}$$

3.4 Model Selection and Model Validation

Model selection is critical for system identification. The focus in this paper are family of function described in the previous section, so model structure is not discussed in not discussed in this paper. The next few sub sections will briefly introduce test the enable selection of model parameter for system identification of ARMAX functions such as delay, number of inputs and outputs.

3.4.1 Determinant Ratio Test

The determinant ratio tests is used to limit the number of possible model order before parameter estimation. [24]. The method is defined in the by the following equations.

$$h_r(n) = (u(t-1)y(k-1)...u(t-n)y(k-n))^T \tag{20}$$

$$H_r(n) = \frac{1}{N}\sum_{t=n+1}^{n+N} h_r(n)h_r^T(n) \tag{21}$$

$$DV(n) = \frac{detH_r(n)}{detH_r(n+1)} \tag{22}$$

The result of the determinant ratio tests is a graph of values (determinant ratio) that will increases as the model order increases. To select the appropriate model from the determinant ratio test, the value that demonstrates a significant increase when compared to the previous value in the candidate model order. This not a precise rule, it serves as a useful guideline [24].

3.4.2 Polynomial Test

The polynomial test involves solving for the poles and zeros of a discrete second order transfer function. The model order is increased for a specific range. The poles and zeros that do not change at the model order increases is known as the characteristic poles and zeros [24][25]. An example of the approach is provided in [25].

3.4.3 Auto-correlation or Independence Test

The key assumption of parameter estimation methods is that the model errors are uncorrelated. To ensure that this assumption holds, the auto-correlation of the errors are calculated using the equation below:

$$R_{\varepsilon\varepsilon}(\tau_N) = \frac{1}{N}\varepsilon(t)\varepsilon(t+\tau_N) \tag{23}$$

3.4.4 Test for Normality

The test for normality is used to check the statistical distribution of the model error. The test for normality can be done using visual methods such as plotting the distribution of the model error using a histogram.

4.0 Study 1: Control Design at Full and Partial Electric Load

4.1 Description of Study & Objectives

In this study, a digital controller is designed using a model identified from open-loop step tests. Two models are developed, each represent the relationship between the fuel valve and turbine speed at two electric loads. During the open-loop step tests the fuel valve position is varied by $\pm 2\%$ from a nominal position. The nominal position depends on the nominal operating conditions of the Hyper facility. A 2% change in the fuel valve position is expected to produce approximately 1000 rpm change in the turbine speed response. The fuel valve step changes last for one minute and each test consists of ten step changes. Figures 8 and 9 illustrate the turbine speed response to changes in the fuel valve position at 50 kW and 25 kW electric load, respectively.

The data from the open-loop step tests are used for system identification. The turbine speed fuel valve (TSFV) relationship is modeled using an ARX model structure. An ARX model structure is chosen because its models outputs as a linear combination of its past outputs (turbine speed) and exogenous inputs (fuel valve). The ARX structure in this study incorporates delay, the amount of time it takes for a given input to appear in the output [26]. In the system it reasonable to assume that a change in the fuel position does not generate a response in the fuel valve in less than the sampling period of 5 millisecond. Recursive least squares is used to determine estimates. A second-order model is used, the parameters for the RLS algorithm are $n_A = n_B = 1$, $\lambda(t) = 1$, and $P_{in} = 1000I$.

Using the identified TSFV transfer function, a digital controller is developed using polynomial pole-placement. The digital controller is designed for regulation and tracking (response to change in command signal). The controller is designed to achieve a desired settling time and percent overshoot. The controller incorporates the integral action, ensuring that the steady-state error of the system is equal to zero. To evaluate the controller, the sensitivity functions are used to evaluate the response of the control action (fuel valve) and output (turbine speed) to changes in a command signal and disturbances.

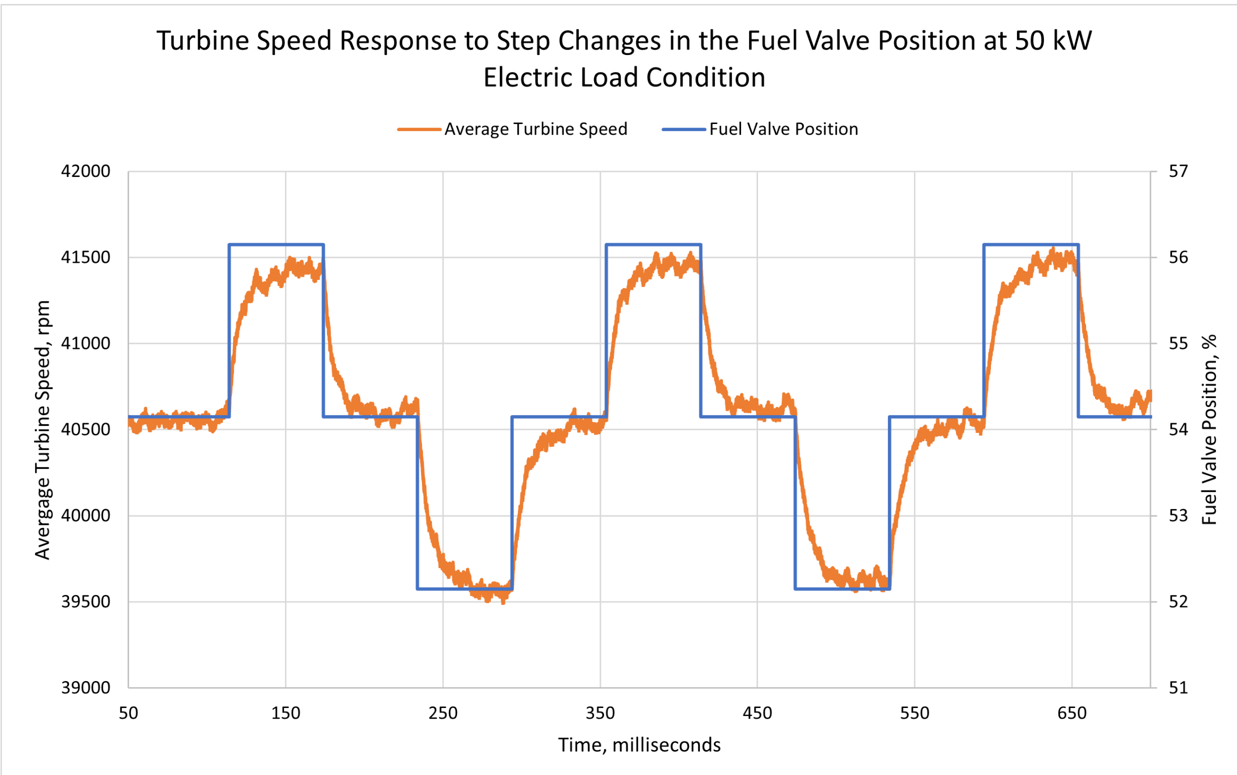

Figure 8: Turbine Speed Response to Open Loop Step Changes in Fuel Valve Position at 50 kW

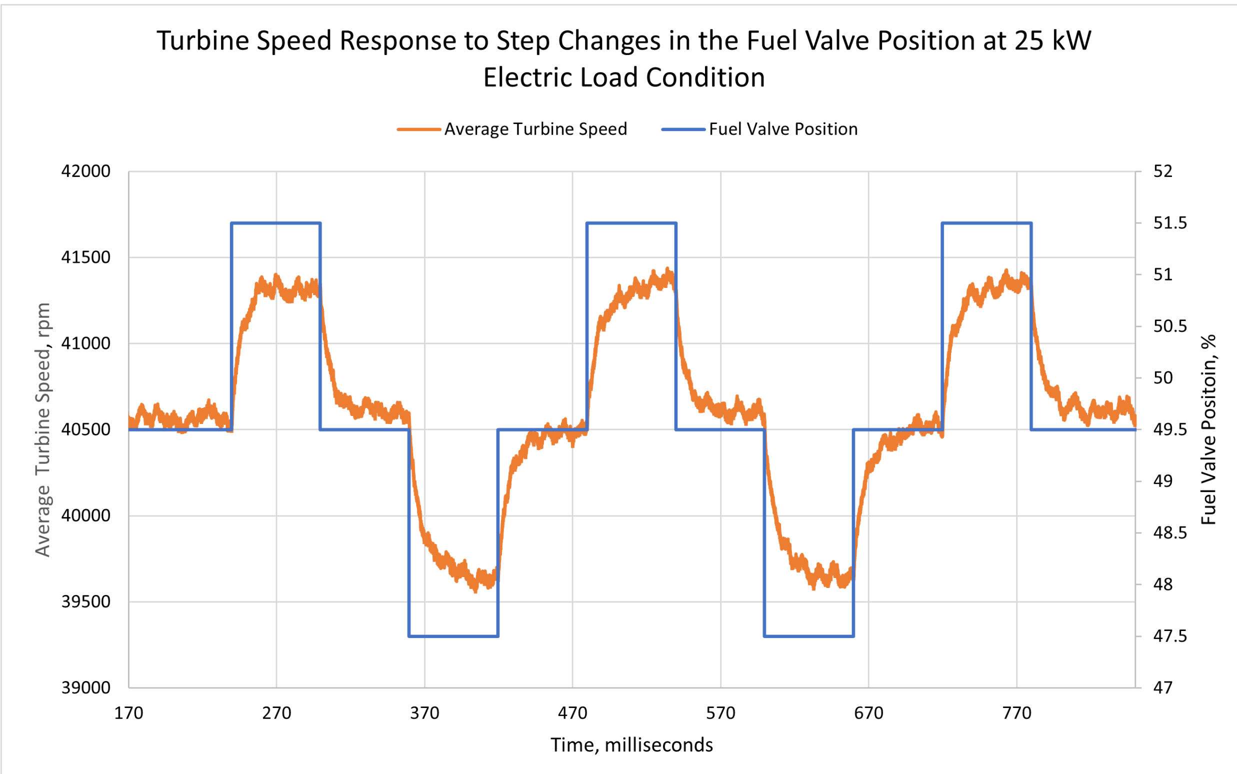

Figure 9: Turbine Speed Response to Open Loop Step Changes in Fuel Valve Position at 25 kW

4.2 System Identification

The turbine speed fuel valve (TSFV) transfer function is developed using an ARX model and RLS. The parameters of the ARX model are as follows; $d = 1$, $n_A = n_B = 2$. The difference equation is

$$y(t) = -a_1 y(t-1) - a_2 y(t-2) + b_1 u(t-2) + b_2 u(t-3)$$

The parameters of the recursive least squares algorithm are $P_{in} = 4000I$ and $\lambda = 1$. The data is normalized between -1 and 1. The fuel valve position is normalized using the nominal fuel valve position and the 2 % step change.

$$\bar{u}_i = \frac{u_i - u_0}{2}$$

where $\bar{u}_i$ is the i^{th} normalized fuel valve position, u_0 is the nominal fuel valve position, and u_i is the i^{th} fuel valve position. The nominal fuel valve positions are 49.5% and 54.5% for 50 kW and 25 kW electric loads, respectively. The turbine speed is normalized using the nominal turbine speed and the maximum expected change in turbine speed due to a 2 % change in the fuel valve, 1000 rpm.

$$\bar{y}_i = \frac{y_i - y_0}{1000}$$

where $\bar{y}_i$ is the i^{th} normalized turbine speed, y_0 is the nominal turbine speed, and y_i is the i^{th} turbine speed. The nominal turbine speed is 40500 rpm and the maximum deviation in turbine speed is 1000 rpm for both electric loads.

The model is identified using 40 % of the experimental data, the remaining data is used to validate the model. Model validation involves using the `lsim` function in MATLAB to predict the turbine speed response given a series of control actions. The residual of the estimation is used to ensure that the residuals are approximately normally distributed and there is no bias in the parameter estimates.

Table 1: Parameter Estimates of the Turbine Speed Fuel Valve Transfer Function

Electric Load	$\hat{a}_1$	$\hat{a}_2$	$\hat{b}_1$	$\hat{b}_2$
50 kW	-0.3929	-0.6056	0.0016	-0.0010
25 kW	-0.4019	-0.5967	0.0059	-0.0048

4.2.1 System Identification Results

The parameter estimates of the TSFV transfer functions at the two electric loads are listed in Table 1. The measured and predicted response of the turbine speed to a series of fuel valve step changes for full and partial electric load are illustrated in Figures 10 and 13, respectively. It can be seen that the identified models in at both operating states has a strong fit with the measured data. The root mean square error for the 50 kW and 25 kW electric loads are 0.8507 and 0.66119, respectively. The frequency of residuals produced by the TSFV was approximately normally distributed as shown in Figures 11 and 14. The TSFV also produced residual values that were uncorrelated. The autocorrelation for the residuals at 50 kW and 25 kW electric loads is presented in Figures 12 and 15. In the autocorrelation plot, the autocorrelation values is plotted against a logarithmic scale of number of data points. Figures 12 and 15, show that it takes approximately 200 data points for the model errors to converge to zero, this is an artifact of the `lsim` function.

4.3 Pole Placement - Polynomial Approach

The polynomial pole placement approach is summarized by the following steps.

1. Identification of process model from data. The polynomials $A(z)$ and $B(z)$ must be coprime.
2. Determine the desired closed-loop $A_c(z)$ and observer $A_o(z)$ polynomials that produce the closed-loop characteristic polynomial $A_{cl}(z)$.

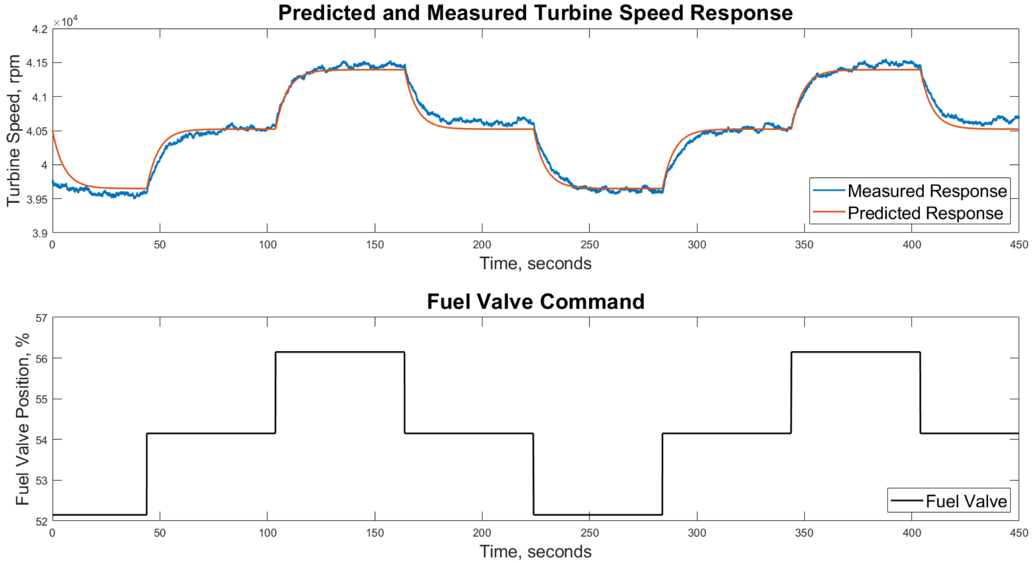

Figure 10: Predicted and Measured Turbine Speed to Fuel Valve Step Changes at 50 kW

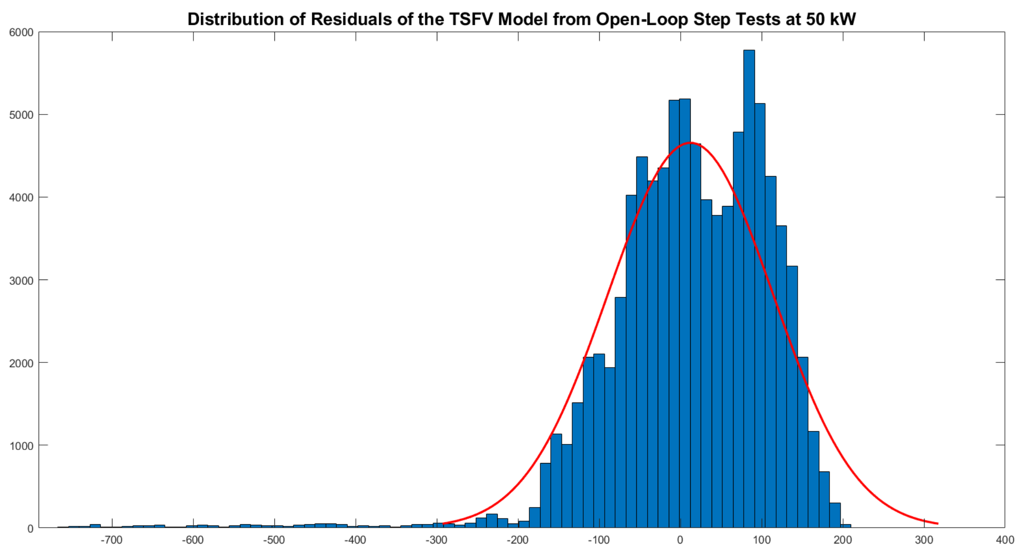

Figure 11: Residual Distribution at 50 kW

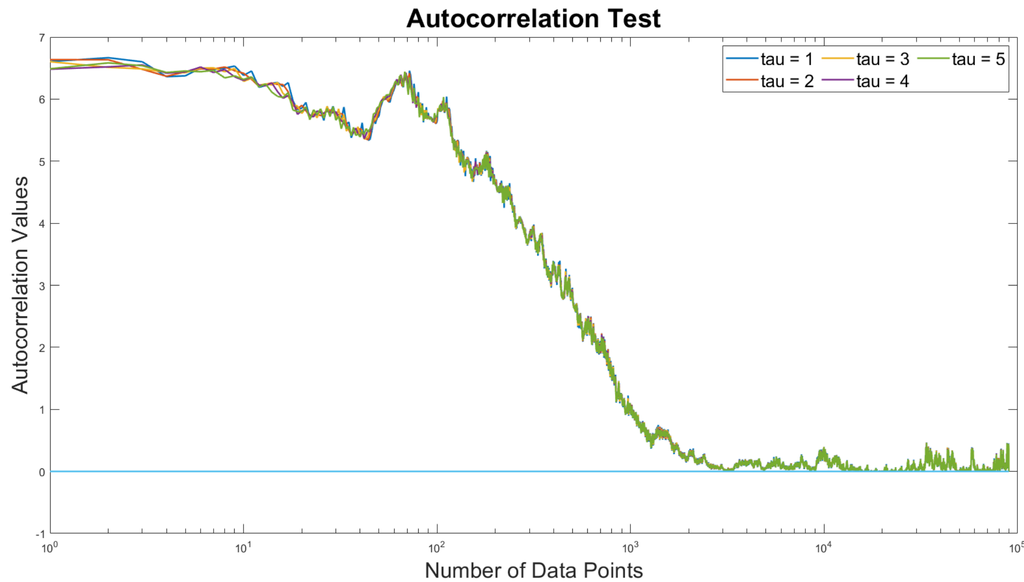

Figure 12: Auto-correlation of Residuals at 50 kW

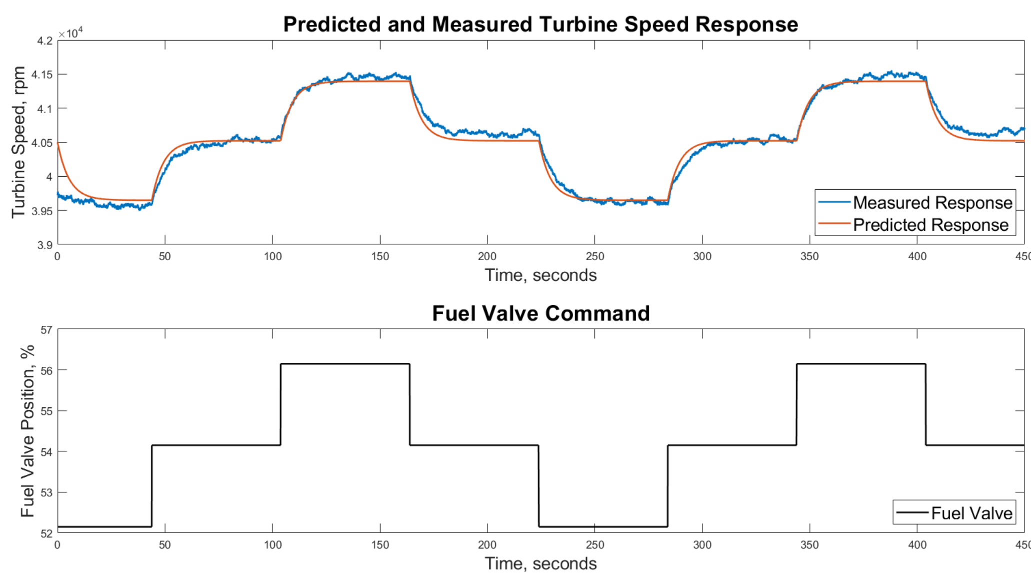

Figure 13: Predicted and Measured Turbine Speed to Fuel Valve Step Changes at 25 kW

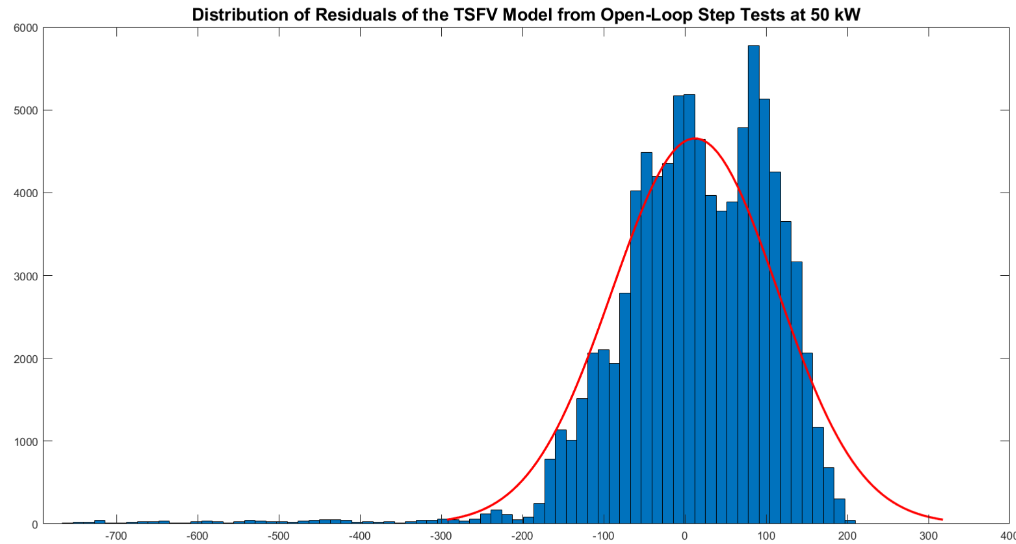

Figure 14: Residual Distribution at 25 kW

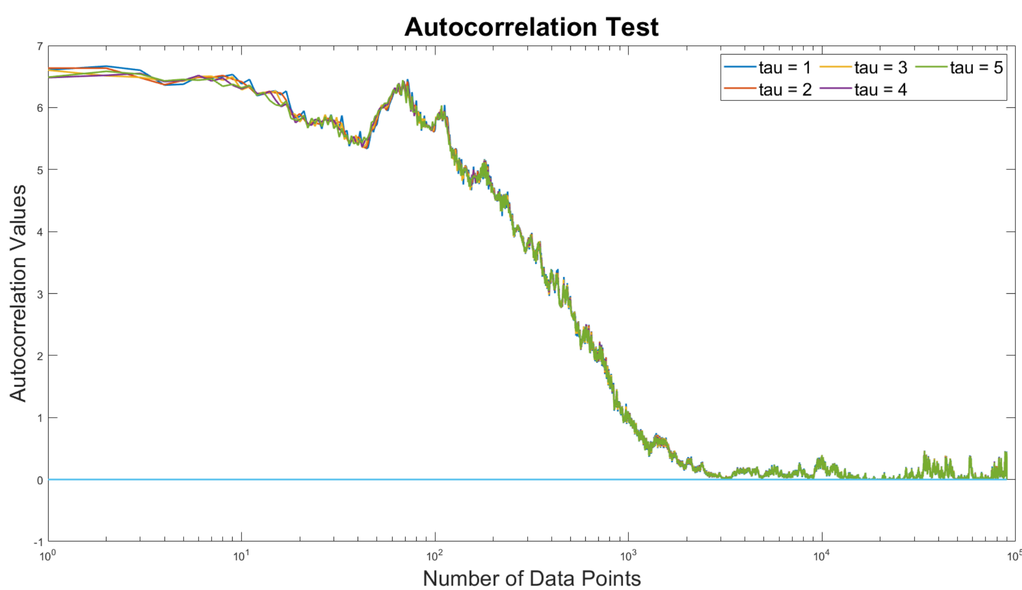

Figure 15: Auto-correlation of Residuals at 25 kW

3. Select $R(z)$ to achieve zero steady state error: $R(z) = (z + r)(z - 1)$
4. Select $S(z)$. In this study, $S(z)$ is selected to be second order.
5. Solve for $R(z)$ and $S(z)$ using the *Diophantine equation*.

Step 1: The turbine speed fuel valve model is identified from open loop step change tests. It has the form

$$G(z) = \frac{\hat{b}_0 z + \hat{b}_1}{\hat{a}_0 z^2 + \hat{a}_1 z + \hat{a}_2}$$

Step 2: The dominant poles of the desired closed-loop response is dependent on the selection of the natural frequency, ω_n, and the damping ratio ζ. The natural frequency and damping ratio define the roots of the continuous-time second order characteristic equation. To solve the digital pole placement problem, a discrete time equivalent of the continuous second order characteristic equation is found using the `c2d` function in MATLAB. It transforms continuous models to discrete time models. The Tustin method is used with a sampling time of 5 ms to determine the discrete-time characteristic equation. In this study, the ideal transient response is one with a fast settling time and minimal overshoot. The controller must produce a transient response with 2 % overshoot and a settling time of 0.75 seconds for both electric loads.

The damping ratio as a function of percent overshoot is

$$\zeta = \sqrt{\frac{\log PO^2}{\pi^2 + \log PO^2}} \tag{24}$$

The natural frequency is a function of the damping ratio and settling time.

$$\omega_n = \frac{4}{t_s \zeta} \tag{25}$$

The discrete time second order transfer function is

$$A_c(z) = z^2 + a_{c1} z + a_{c2}$$

A second order observer is designed to achieve a controller with integral action [14]. The observer is selected as the discrete time equivalent of the continuous time equation

$$G(s) = \frac{1}{(s + a)^2} \tag{26}$$

There are two poles at $s = -a$. The discrete time equation 26 is

$$A_o(z) = (z - e^{-aT_s})^2 = z^2 + a_{o1}z + a_{o2} \tag{27}$$

where T_s is the sampling period. The observer poles can also be defined by choosing a natural frequency and damping ratio much like the characteristic equation to attain the dominant poles. The observer poles impact the response of to disturbances and measurement noise. For example, to reduce measurement noise the observer poles are selected to be slower. The response to disturbances is impacted by choosing a observer poles that produces a delay in observing the disturbance, thus selection of sampling period can improve response to disturbances. [**?**]. Rules for selecting sampling periods and observer poles are provided in [**?**]. In this study, the sampling period of the controller is five milliseconds. For both electric loads, $a = 275$.

Step 5: To solve for the polynomials $R(z)$ and $S(z)$, observer and controller polynomials are factored.

$$A_{cl}(z) = z^4 + (a_{o1} + a_{c1})z^3 + (a_{o2} + a_{c1}a_{o1} + a_{c2})z^2 + (a_{c1}a_{o2} + a_{c2}a_{o1})z + a_{c2}a_{o2}$$

The digital controller is achieved by solving the following equation

$$A(z)R(z) + B(z)S(z) = A_{cl}(z)$$

After factoring the polynomials, the following system of equations is found

$$a_0r_0 = 1$$

$$a_1r_0 + a_0r_1 + b_0s_0 = a_{o1} + a_{c1}$$

$$a_2r_0 + a_1r_1 + a_2r_2 + b_1s_0 + b_0s_1 = a_{o1} + a_{c1}$$

$$a_2r_1 + a_1r_2 + b_1s_1 + b_0s_2 = a_{c1}a_{o2} + a_{c2}a_{o1}$$

$$a_2r_2 + b_1s_2 = a_{c2}a_{o2}$$

Table 2: $R(z)$ and $S(z)$ Coefficients of the Turbine Speed Fuel Valve Controller

Electric Load	r_0	r_1	r_2	s_0	s_1	s_2
50 kW	1.000	-1.6336	0.5417	-26.2631	200.6800	-173.5683
25 kW	1.000	-1.9499	0.8907	-17.0409	141.5445	-123.8704

Table 3: $T(z)$ Coefficients of the Turbine Speed Fuel Valve Controller

Electric Load	t_0	t_1	t_1
50 kW	0.8822	-0.1488	0.0059
25 kW	1.0030	-0.5072	0.0641

The linear equation can be represented at a matrix equation $Mx = p$ where p is the desired closed-loop poles. M is the *Sylvester matrix* and x is a vector containing the controller coefficients. The linear matrix equation is

$$\begin{bmatrix} a_0 & 0 & 0 & 0 & 0 & 0 \\ a_1 & a_0 & 0 & b_0 & 0 & 0 \\ a_2 & a_1 & a_0 & b_1 & b_0 & 0 \\ 0 & a_2 & a_1 & 0 & b_1 & b_0 \\ 0 & 0 & a_2 & 0 & 0 & b_1 \end{bmatrix} \begin{Bmatrix} r_0 \\ r_1 \\ r_2 \\ s_0 \\ s_1 \\ s_2 \end{Bmatrix} = \begin{Bmatrix} 1 \\ a_{o1} + a_{c1} \\ a_{o2} + a_{c1}a_{o1} + a_{c2} \\ a_{c1}a_{o2} + a_{c2}a_{o1} \\ a_{c2}a_{o2} \end{Bmatrix}$$

4.3.1 Pole Placement Results

The controller coefficients determined from solving the *Diophantine equation* are listed in Table 2 and 3. Table 2 lists the coefficients of the polynomials $R(z)$ and $S(z)$. Table 3 lists the coefficients of the polynomial $T(z)$.

The response of the closed-loop system to changes in the command and disturbance signal is evaluated using four sensitivity functions: output - command signal, output - disturbances, control action - command signal, and control action - disturbances . Equation 28 lists the sensitivity function in that order [14].

$$
\begin{aligned}
y &= \frac{B(z)T(z)}{A(z)R(z)+B(z)S(z)}r(t) \\
y &= \frac{A(z)R(z)}{A(z)R(z)+B(z)S(z)}e(t) \\
u &= \frac{A(z)T(z)}{A(z)R(z)+B(z)S(z)}r(t) \\
u &= \frac{A(z)S(z)}{A(z)R(z)+B(z)S(z)}e(t)
\end{aligned}
\tag{28}
$$

Figure 16 and 19 show the turbine speed and fuel response to a step change in the turbine speed command at 50 kW and 25 kW electric load, respectively. The turbine speed response has a rise time of 0.35 seconds, a settling time of 0.74 seconds, and an overshoot of 2.01 % at 50 kW. The turbine response at 25 kW electric load has a rise time of 0.3450, a settling time of 0.74 seconds, and a slightly larger overshoot, 2.03%. The change in the fuel valve position due to a 200 rpm increase in turbine speed is approximately 0.7 at both electric loads.

Figures 17 and 20 show the turbine speed and fuel valve response to disturbance that increases turbine speed by 100 rpm. The 100 rpm is the typical change in the turbine speed when the electric load is changed by 5 kW. In both figures, the increase in turbine speed causes the fuel valve position to decrease immediately by approximately 0.5%. After the instantaneous decrease in the fuel valve position, the fuel valve overshoots, before settling at its new nominal position. The turbine speed at 50 kW and 25 kW settles a slightly lower speed after a disturbance in introduced. This is expected because fuel does not return to it original position. The increase in the turbine speed is due to an increase in electric load, which results in a increase in the turbine speed, the fuel valve compensates falling immediately, rises to bring the system the turbine speed to nominal speed of 40500 rpm. Ideally, the turbine speed and fuel valve would return to its nominal speed and rotation.

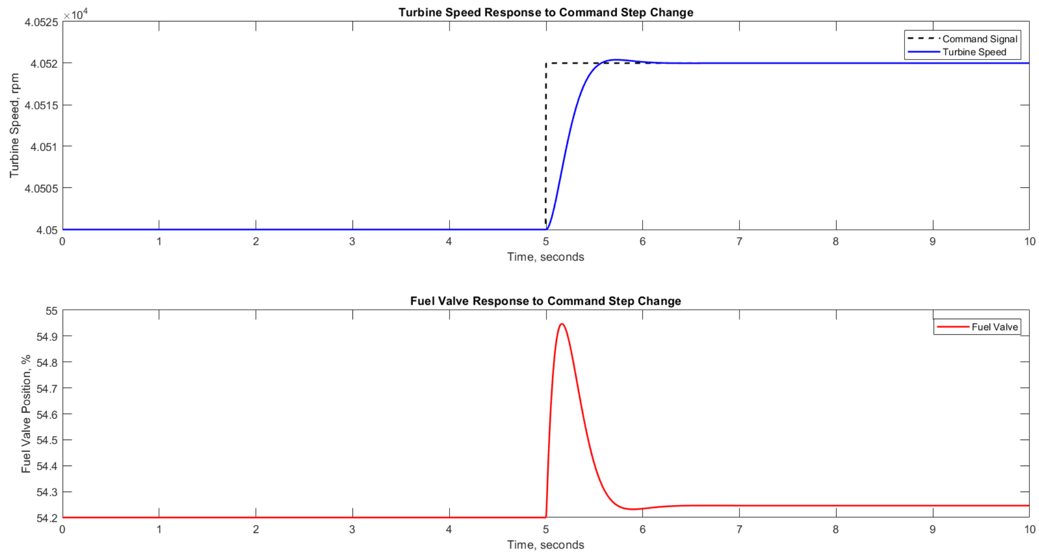

Figure 16: Turbine speed and fuel valve response to a 200 rpm change in turbine speed command at 50 kW electric load

This indicates that the better disturbance rejection is required. Disturbance rejection can be improved by selecting better observer poles or changing the sampling frequency of the controller [14].

Figures 18 and 21 show the turbine speed and fuel valve response to step changes in the command signal and random disturbances. The disturbances are withing the range of 40500 $\pm$ 100 rpm. The turbine speed response to changes in the command signal was promising because the system achieved the desired responses. Although, during operation, the turbine speed is not controlled directly, the results indicate that it is possible to use the controller for turbine speed following. It is very unlikely that the developed controller will be used to ramping during start-up or shutdown. A different controller will need to be designed to achieve the desired ramp rates; however, the pole-placement approach can be used to achieve a controller suitable for ramping operations. The regulation and tracking dynamics will need to be defined separately, unlike the control designed used in this study. The error driving this controller in study is the difference between the command, $r(t)$, and the output $y(t)$.

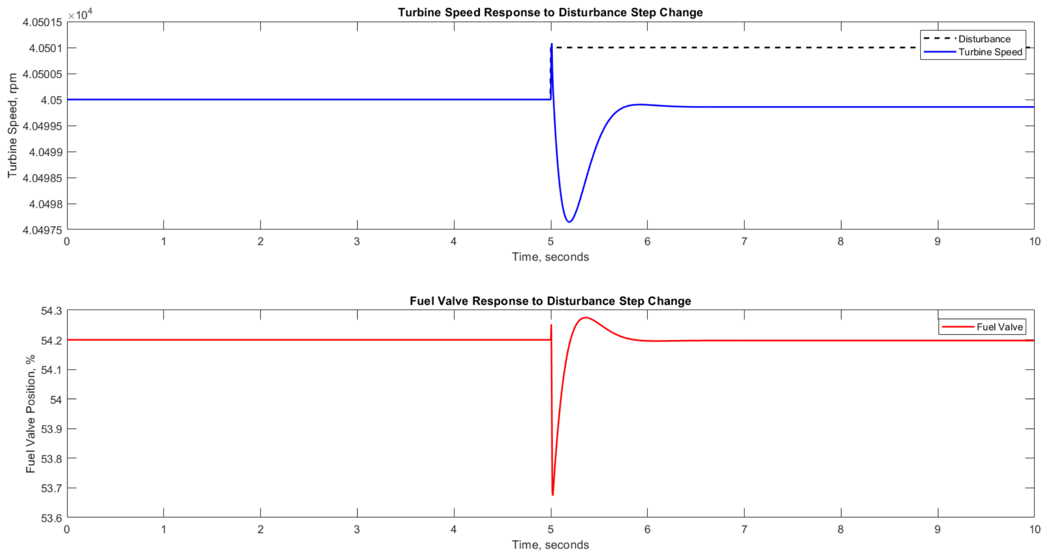

Figure 17: Turbine speed and fuel valve response to a step change in disturbance at 50 kW electric load

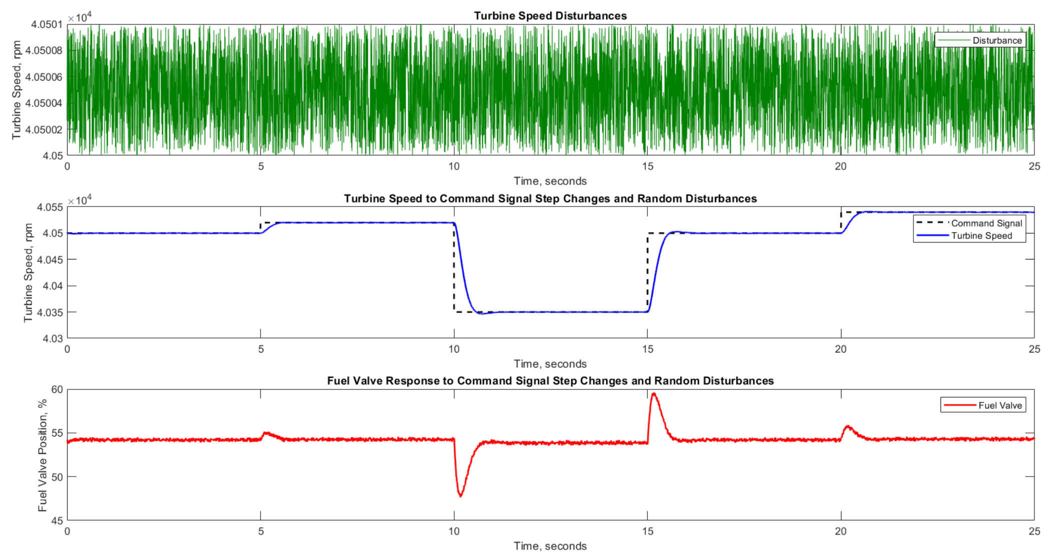

Figure 18: Turbine speed and fuel valve response to step changes in turbine speed command and random disturbances at 50 kW Electric Load

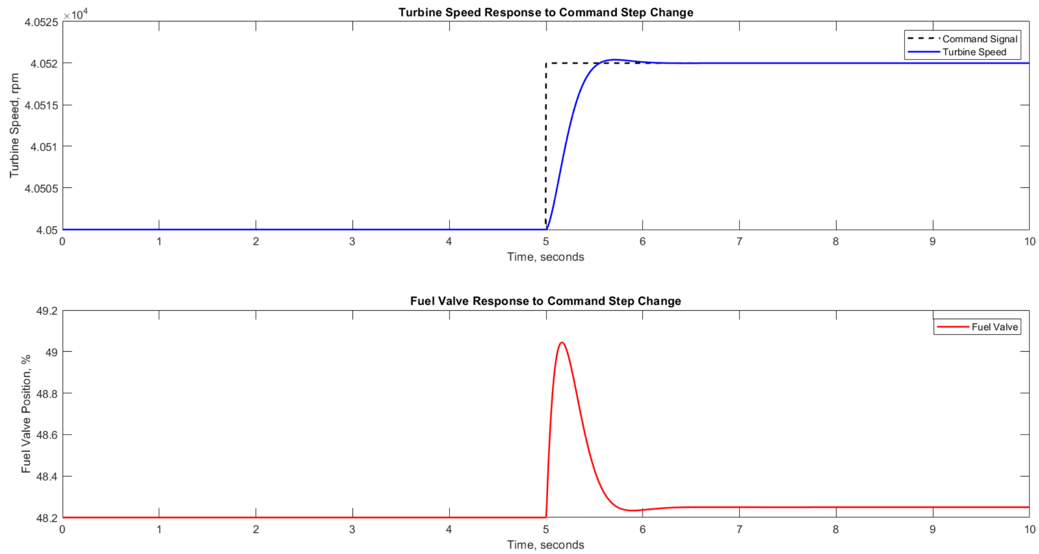

Figure 19: Turbine speed and fuel valve response to a 200 rpm change in turbine speed command at 25 kW electric load

To determine the robustness of the controller, that is the sensitivity of the controller to various errors, the transfer function

$$\mathcal{L} = \frac{B(z)S(z)}{A(z)R(z)} \tag{29}$$

is used to determine the measures of robustness such as gain, phase, delay, and modulus margin.

The frequency response of transfer $\mathcal{L}$ at both electric loads is provided in Figures 22 and 23.

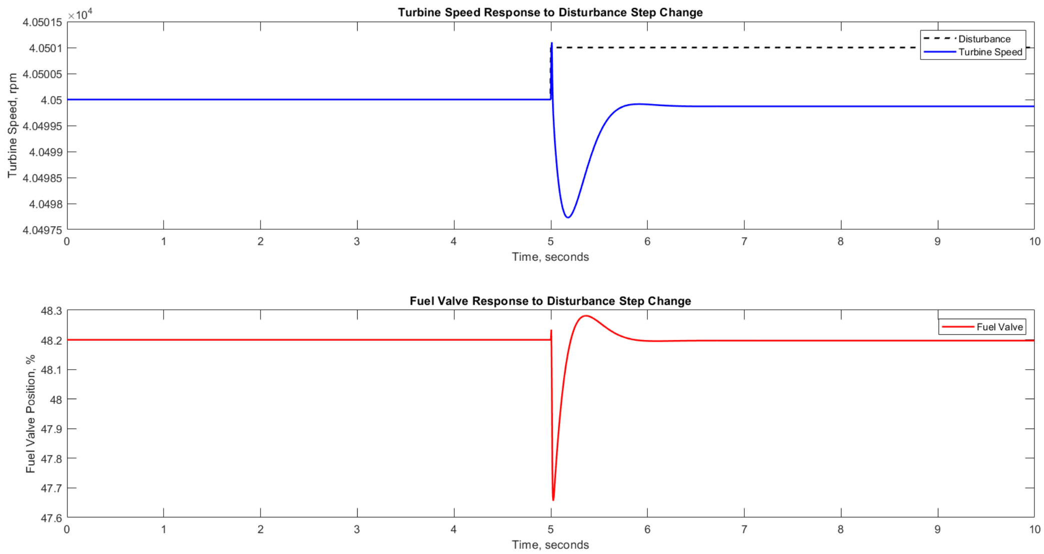

Figure 20: Turbine speed and fuel valve response to a step change in disturbance at 25 kW electric load

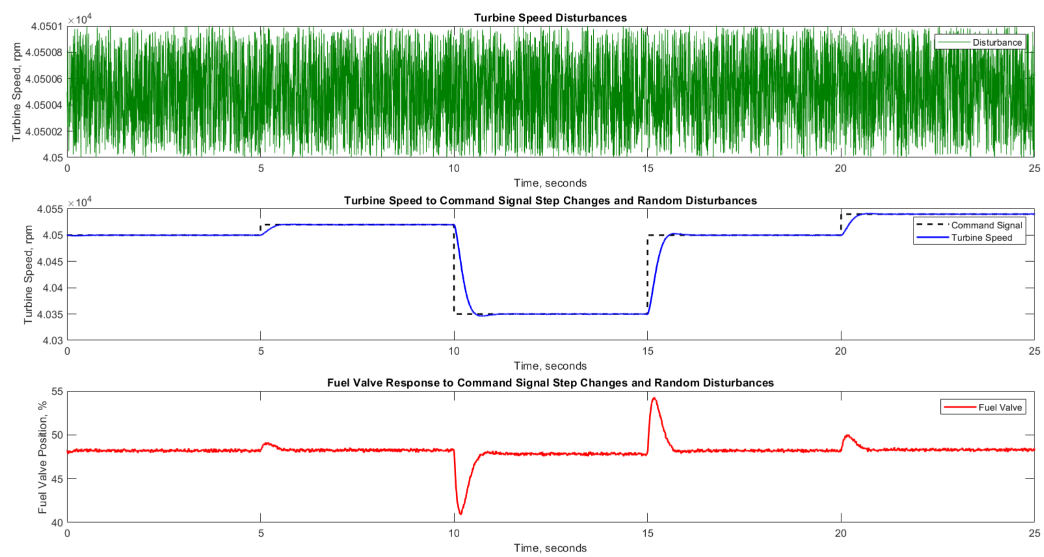

Figure 21: Turbine speed and fuel valve response to step changes in turbine speed command and random disturbances at 25 kW electric load

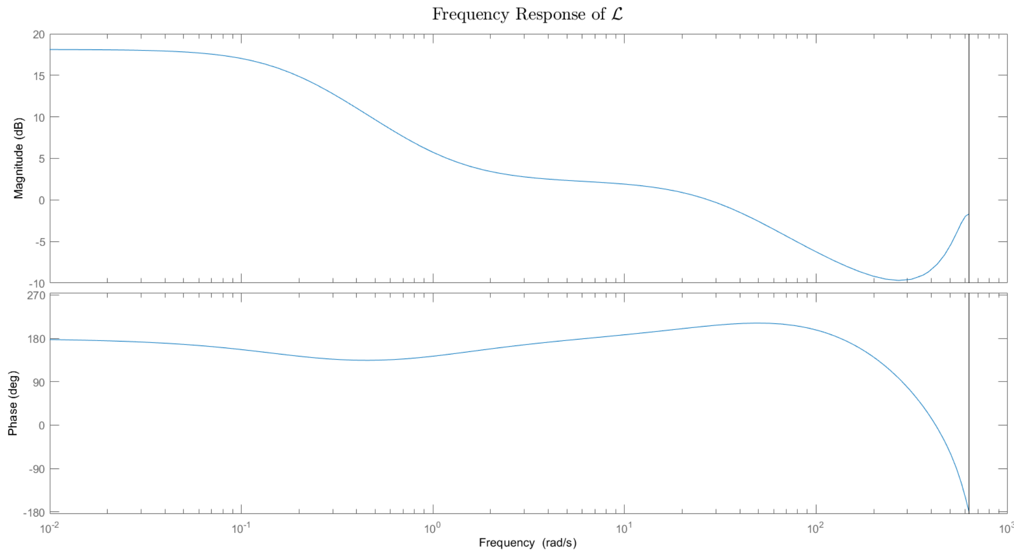

Figure 22: Frequency Response of $\mathcal{L}$ at 50 kW Electric Load

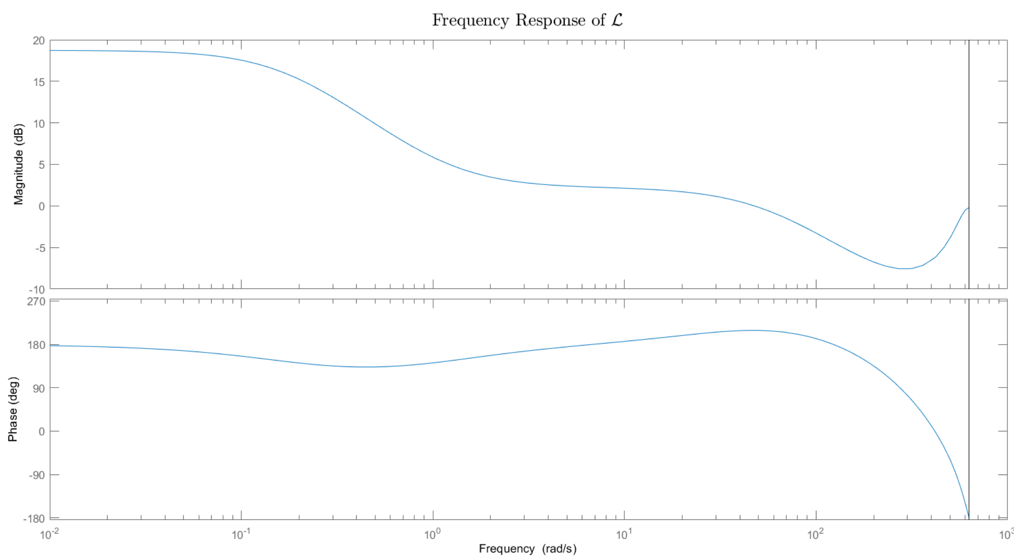

Figure 23: Frequency Response of $\mathcal{L}$ at 25 kW Electric Load

5.0 Study 2: Evaluation of Adaptive Pole Placement with varying Cold Air Bypass Valve Position and Electric Load

5.1 Description of Study & Objectives

This study is concerned with closed-loop identification of the turbine speed fuel valve transfer function model with varying electric load and cold-air bypass valve positions. This study used open-loop data to develop a fuel valve transfer function model. The open-loop step change test was conducted at 40 kW electric load and cold air bypass valves at 40%. The ARX structure is used and recursive least squares is used for parameter estimation. The approach and parameters used to develop a TSFV from open-loop data in Study 1 is still valid. The identified model is used to develop a digital controller using the pole placement approach. The controller has the same objectives as the controller designed in Study 1.

The disturbance models used in this study are developed closed-loop step change tests. The disturbance models are identified from four operating states based on the combination of the electric load and cold-air bypass valve positions. The four states are as follows: 40 kW & 40 %, 40 kW & 20 %, 20 kW & 20 %, and 20 kW & 40 %. The disturbance model of interest describes the impact of a 5 kW step change in the electric load on the turbine speed. An increase in the electric load decreases the turbine speed, resulting in an increase the fuel valve position to maintain a nominal turbine speed of 40500 rpm. The disturbance model is treated as an ARMAX model and a recursive extended least squares algorithm is used for parameter estimation.

After identifying the plant and disturbance algorithm, a Simulink model is created to understand how the turbine speed responses to disturbances under feedback control. The predicted turbine speed response and fuel valve is ignored in this study. This study primarily concerned with the direct identification using recursive extended least squares. The aim is to identify the changes in the plant model due variations in the turbine speed caused by changes in the electric load. The second aim of this study to estimate the plant model from the closed-loop model in Simulink. The model identified from the simulated closed-loop system is compared to the models identified from open-loop and closed-loop tests performed in the experimental facility. The impact of noise on online system identification is explored as well the impact of initial selection of parameter estimates and choice of forgetting factor.

5.2 System Identification - Disturbance Model

The turbine speed electric load (TSEL) transfer function is developed using an ARMAX structure and a RELS algorithm for parameter estimation. The parameters of the ARMAX structure are as follows; $d = 1$, $n_A = n_B = n_C = 2$. This produces the following difference equation

$$y(t) = -a_1 y(t-1) - a_2 y(t-2) + b_1 u(t-2) + b_2 u(t-3)$$

The parameters of the recursive extended least squares algorithm are as follows; $P_{in} = 4000I$,$\lambda = 1$. The data is normalized between -1 and 1. The electric load is normalized using the nominal electric load and the 5 kW step change.

$$\bar{u}_i = \frac{u_i - u_0}{2}$$

where $\bar{u}_i$ is the i^{th} normalized fuel valve position, u_0 is the nominal fuel valve position, and u_i is the i^{th} fuel valve position.

The turbine speed is normalized using the nominal turbine speed and the maximum expected change in turbine speed due to a ±5 kW change in the electric load is approximately 100 rpm.

$$\bar{y}_i = \frac{y_i - y_0}{1000}$$

where $\bar{y}_i$ is the i^{th} normalized turbine speed, y_0 is the nominal turbine speed, and y_i is the i^{th} turbine speed. The nominal turbine speed in 40500 rpm and the maximum deviation is 100 rpm for both electric loads.

The model is identified using 40 % of the experimental data, the remaining data is used to validate the model. Model validation involves using the `lsim` function in MATLAB to predict the turbine speed response given a series of control actions. The distribution of the error predicted and measured turbine speed response, the residual, is plotted to ensure that the distribution is normal. The auto correlation of the residual is calculated to ensure there is no bias in the parameter estimates.

5.3 Simulink Model

A Simulink model used to study the impacts of the electric load disturbance on the the turbine speed response. The model consists of a two degree of freedom controller designed using the pole-placement approach, a TSFV transfer function identified from open-loop data, and an electric load disturbance model identified from closed-loop data. The input of the electric load disturbance model are step changes. Increasing the electric load decreases the turbine speed. A band limited white noise generator is included in the system as well.

5.4 Adaptive Pole Placement Control

Direct identification is a closed-loop system identification strategy that treats the controller an unknown entity, it strictly considers the output of the controller and the response of the plant. To identify the TSFV from closed-loop data, a recursive extended least squares algorithm is used. An ARMAX model is used to identify the TSFV transfer function. The fuel valve position and turbine speed are the input and output data used to identify the TSFV transfer function. The initial parameters of the RELS algorithm: $n_A = n_B = n_C = 2$, $d = 1$, and $\hat{\theta} = [-0.4265, -0.5722, 0.002226, -0.001682, 0.358, 0.458]^T$. Controller estimates are calculated every five milliseconds by solving the *Diophantine equation*.

Figure 24 compares the frequency response of the plant and identified TSFV transfer functions in a noisy and noiseless environment. The noise is added as a disturbance. It can be seen in Figure 19 that the estimated model from the noisy environment had a magnitude and phase response closed to that of the plant. The estimated model from the noiseless environment has a magnitude response that was noticeably different from the plant.

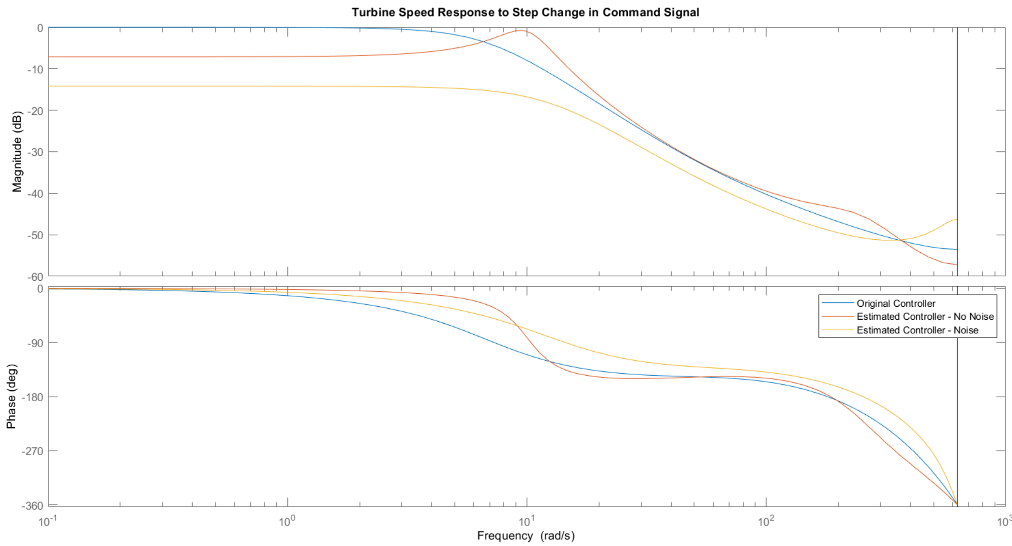

Figure 24: Frequency Response of the Plant and Identified Turbine Speed Fuel Valve Transfer Functions

Figure 25 illustrates the effect of noise on updating controller coefficients. The updating coefficients of the controller polynomials $R(z)$ and $S(z)$ in the noisy environment experienced no sudden changes when the disturbances were introduced to the controller. This is due to constant excitation caused by the addition of band-limited white noise in the Simulink model. In coefficients of the controller in the noiseless environment experienced periodic spikes in the controller when a disturbance was introduced. These spikes in the controller parameters when implemented in the system may causes instability in the closed-loop system.

Figure 26 shows the step response of a closed-loop system of three systems. The first closed-loop step response is based on the controller designed from the plant model. The second closed-loop step response is based on the controller estimated from closed-loop system with band limited white noise. The third closed-loop step response is based on the controller estimated from closed-loop system with no band limited white noise. The original controller is designed to achieve a settling time of 0.75 seconds and 2% overshoot. The closed-loop response with no noise has a settling time of 1.40 seconds and 45.0% overshoot. The closed-

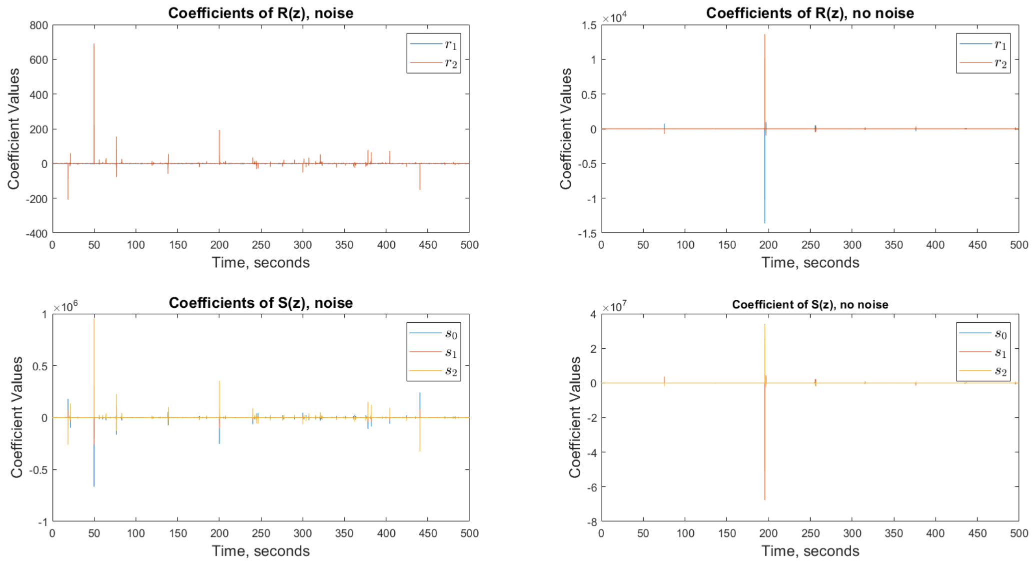

Figure 25: Updating Coefficients of the Controller Polynomials $R(z)$ and $T(z)$ in Noise and Noiseless Disturbance

loop response of the system with no noise has a settling time of 0.30 seconds and 1.07% overshoot.

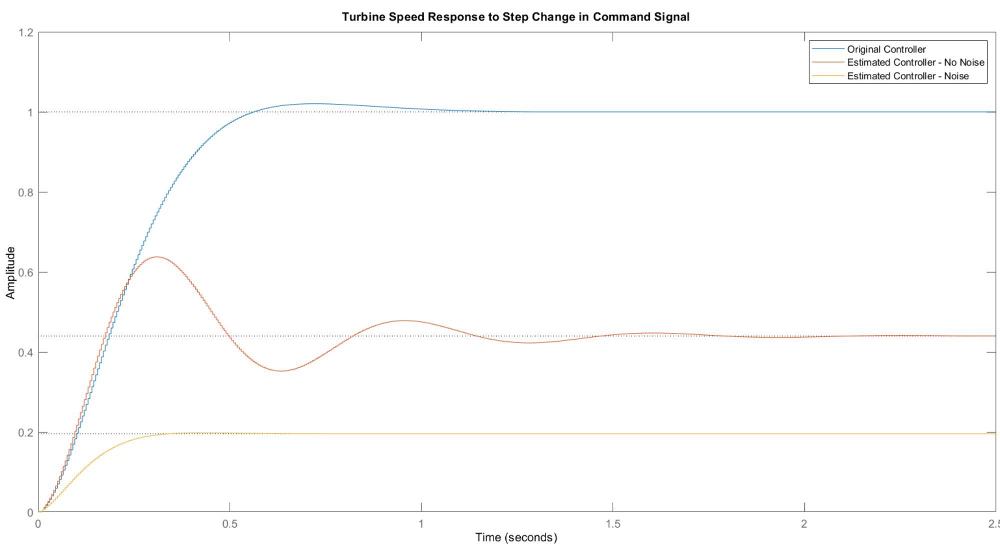

Figure 26: Step Response of the Plant and Identified Turbine Speed Fuel Valve Transfer Functions

6.0 Conclusions and Discussion

Closed-loop system identification using data from the experimental facility remains an issue. It did not produce an model suitable for control design. Using the direct identification approach it is not possible to identify a model with similar time domain and frequency from closed-loop data.

It is interesting to note that closed-loop system identification from the simulation was able to produce a model with similar time domain and frequency responses. The closed-loop simulation in Simulink only involves only a turbine speed fuel valve and the electric load turbine transfer functions, the plant and disturbance models respectively. The discrepancies in the transfer functions is likely due to the effect of other processes. When the electric load command is changed is does not only effect the turbine speed, it effects can be observed in mass flow rate, temperature, and pressure measurements in the system. Improving closed-loop identification will require using more measurements; from a modeling aspect, more degrees of freedom are required to accurately model the fuel valve turbine speed relationship when a disturbance is introduced. The ARMAX structure discussed in this work can be used for system identification of multi-input, single output systems. The recursive least squares algorithm will need to need to be modified for the higher degree of freedom system. Only parameter estimates for the turbine speed fuel valve relationship will be used. Despite inability to attain a plant model from the closed-loop step change implemented in the Hyper facility, closed-loop identification still remains promising, and is of vital importance for developing self-tuning regulators. Single-input, single-output models are inadequate and multi-input structure should be explored to improve identification. The ARMAX structure can be modified to a multiple input, multiple output structure, adding more degrees of freedom. Process parameters like temperature, pressure, and mass flows and their effect of temperature can be included to improve closed-loop system identification. The recursive extended least squares algorithm can be used for parameter estimation of the proposed MISO-ARMAX model [27].

Beyond the polynomial models, neural networks may be a possible approach to closed-loop system identification. For offline closed-loop system identification, the neural network can be effective in identifying processes with nonlinear dynamics. However, its applicability in a self-tuning regulator remains an issue. The model identified by the neural network will only work in the for a single operating condition. The neural network can not be safely trained in an online manner to produce parameter estimates to self-tuning regulation [11]. The issue of safe online learning (online system identification) is an open of research.

Another possible explanation of the failure of direct identification to produce a good model, model that produces a viable controller, is that the data used did not contain enough frequencies. It failed to meet the persistent excitation criteria. Future closed-loop step tests will require randomization of the disturbances to produce data that contains enough frequencies for identification purposes.

Open-loop system identification was very successful. It produced models that closely matched the measured response in the experimental facility. A stable and robust controller was attainable from open-loop system identification. Using the model developed from open-loop system identification it was possible to simulate a closed-loop response that matched the experimental data from the Hyper using the turbine speed fuel valve model (developed from open-loop data) and the electric load disturbance model (developed from closed-loop data). This closed-loop simulation was used to determine the feasibility of updating controller coefficients.

Online parameter estimation or online system identification using the recursive extended least squares algorithms was able to identify an adequate plant model in the Simulink simulation. A key feature to note for implementation is the selection of the initial parameter estimates and forgetting factor. The RELS took more than 100s to converge when the initial parameters were zero; however, convergence speed was improved when the coefficients of the plant where non-zero. The convergence improved as the initial parameter estimates approached the true parameter estimates of the plant. The selection of the forgetting factor was also critical to the performance of online system identification. The forgetting factor informs the algorithm on how to value information; whether to bias towards past or current measurements. This study used a variable forgetting factor that used the residuals to change the value of the forgetting factor. The variable forgetting factor performed poorly compared to a forgetting factor of unity. The forgetting factor used was used in online parameter estimation of an self-tuning regulator for an inverter

The effect of noise, introduced as an additional disturbance in the system, had the effect of reducing the effect of bursting in the system. Bursting is a phenomena by which parameter estimates change in a manner that destabilized the closed-loop system due to under excitation in the adaptive feedback loop. [28]. In this system, the parameter estimates are well behaved when the control error is zero, when an disturbance is introduced in the system this can force the parameters into instability. Typically the bursting phenomena is avoided by turning off the adaptation algorithm during steady-state operation. Another possible resolution to preventing bursting is to introduce a small excitation into the system on a set-point (command) signal [29].

Other problems beyond bursting will apply to the application of adaptive control in the SOFC-GT system: transient instability, unstable closed-loop poles, and changing conditions are discussed briefly in [30].

Error based parameter estimation can be replaced by observer inspired online parameter estimation techniques. The benefit of the observer inspired approach is the guarantee of exponential convergence of the parameter estimates. Online parameter estimation based on recursive algorithms are dependent on their initial conditions as previously mentioned and can be time-consuming. The RLS algorithm used in the Hyper facility takes 300 seconds to converge, this will inhibits the development of an adaptive controller to facilitate rapid load changes. The convergence times needs to improve [31]. Observer based approaches can improve the convergence time. Zhang et al. have proposed a sliding mode observer (SMO) that that with fast response and error convergence [32]. Sliding mode observers provide a promising alternative to recursive estimation algorithms.

Pole-placement design using the polynomial approach was successful in both studies, the desired performance was achieved. Other control design techniques like stochastic, sliding mode, extremum seeking, linear quadratic, and model-predictive control [10][13].

7.0 Acknowledgements

I would like to express my deepest appreciation to the Hybrid Performance Project team at NETL, Dr. David Tucker, Dr. Larry Shaddle, Dr. Nor Farida Harun, Dr. Nana Zhou, and Dr. Biao Zhang, for their contributions. I am also thankful for the assitance of Dr. Daniel Cole and Dr. William Clark for their input and suggestions. This endeavor would not have been possible without the mentorship, support, and advice of Dr. Nikhil Bajaj.

Bibliography

[1] S. Impram, S. Varbak Nese, and B. Oral, "Challenges of renewable energy penetration on power system flexibility: A survey," *Energy Strategy Reviews*, vol. 31, p. 100539, 2020.

[2] F. Alobaid, N. Mertens, R. Starkloff, T. Lanz, C. Heinze, and B. Epple, "Progress in dynamic simulation of thermal power plants," *Progress in Energy and Combustion Science*, vol. 59, pp. 79–162, 2017.

[3] O. Prokhorov and D. Dreisbach, "The impact of renewables on the incidents of negative prices in the energy spot markets," *Energy Policy*, vol. 167, p. 113073, 2022.

[4] M. Baqir Hashmi, M. Mansouri, and M. Assadi, "Dynamic performance and control strategies of micro gas turbines: State-of-the-art review, methods, and technologies," *Energy Conversion and Management: X*, vol. 18, p. 100376, 2023.

[5] M. A. Azizi and J. Brouwer, "Progress in solid oxide fuel cell-gas turbine hybrid power systems: System design and analysis, transient operation, controls and optimization," *Applied Energy*, vol. 215, pp. 237–289, 2018.

[6] D. A. Tucker, N. F. Harun, and L. J. Shadle, "Solid oxide fuel cell-gas turbine hybrid power systems: Load following capability for microgrid applications," 6 2018.

[7] A. Buonomano, F. Calise, M. D. d'Accadia, A. Palombo, and M. Vicidomini, "Hybrid solid oxide fuel cells–gas turbine systems for combined heat and power: A review," *Applied Energy*, vol. 156, pp. 32–85, 2015.

[8] B. Zhang, D. Maloney, N. Farida Harun, N. Zhou, P. Pezzini, A. Medam, R. Hovsapian, S. Bayham, and D. Tucker, "Rapid load transition for integrated solid oxide fuel cell – gas turbine (sofc-gt) energy systems: A demonstration of the potential for grid response," *Energy Conversion and Management*, vol. 258, p. 115544, 2022.

[9] *A Real-Time Spatial SOFC Model for Hardware-Based Simulation of Hybrid Systems*, vol. ASME 2011 9th International Conference on Fuel Cell Science, Engineering and Technology of *International Conference on Fuel Cell Science, Engineering and Technology*, 08 2011.

[10] W. S. Black, P. Haghi, and K. B. Ariyur, “Adaptive systems: History, techniques, problems, and perspectives,” *Systems*, vol. 2, no. 4, pp. 606–660, 2014.

[11] A. M. Annaswamy and A. L. Fradkov, “A historical perspective of adaptive control and learning,” *Annual Reviews in Control*, vol. 52, pp. 18–41, 2021.

[12] K. Åström and B. Wittenmark, *Adaptive Control (1 ed.)*. Addison-Wesley, 1989.

[13] I. D. Landau, R. Lozano, M. M'Saad, and A. Karimi, *Apadtive Control*. Springer London, 2011.

[14] K. J. Åström and B. Wittenmark, *Computer-Controlled Systems (3rd Ed.)*. USA: Prentice-Hall, Inc., 1997.

[15] A. Casanova, “A consortium approach to commercialized westinghouse solid oxide fuel cell technology,” *Journal of Power Sources*, vol. 71, no. 1, pp. 65–70, 1998.

[16] F. Jurado and J. R. Saenz, “Adaptive control of a fuel cell-microturbine hybrid power plant,” *IEEE Transactions on Energy Conversion*, vol. 18, no. 2, pp. 342–347, 2003.

[17] *Advanced Power System Development using Cyber-Physical Components Integrated in Gas Turbine Cycle*, Sustainable PolyEnergy generation and HaRvesting, 09 2019.

[18] *Cyber-Physical Systems: A New Paradigm for Energy Technology Development*, vol. Volume 1: Fuels, Combustion, and Material Handling; Combustion Turbines Combined Cycles; Boilers and Heat Recovery Steam Generators; Virtual Plant and Cyber-Physical Systems; Plant Development and Construction; Renewable Energy Systems of *ASME Power Conference*, 06 2018.

[19] B. SA, *Nonlinear System Identification : NARMAX Methods in the Time, Frequency, and Spatio-Temporal Domains*. John Wiley Sons, Incorporated, 2013.

[20] M. Gevers, “Identification for control: From the early achievements to the revival of experiment design*,” *European Journal of Control*, vol. 11, no. 4, pp. 335–352, 2005.

[21] U. Forssell and L. Ljung, “Closed-loop identification revisited,” *Automatica*, vol. 35, no. 7, pp. 1215–1241, 1999.

[22] L. Ljung, “Identification in closed loop: Some aspects on direct and indirect approaches,” *IFAC Proceedings Volumes*, vol. 30, no. 11, pp. 155–160, 1997. IFAC Symposium on System Identification (SYSID’97), Kitakyushu, Fukuoka, Japan, 8-11 July 1997.

[23] L. Ljung, *System Identification: Theory for the User*. Prentice Hall, 1999.

[24] H. Unbehauen and B. Göhring, “Tests for determining model order in parameter estimation,” *Automatica*, vol. 10, no. 3, pp. 233–244, 1974.

[25] T. Söderström, “Test of pole-zero cancellation in estimated models,” *Automatica*, vol. 11, no. 5, pp. 537–539, 1975.

[26] I. Landau, “The r-s-t digital controller design and applications,” *IFAC Proceedings Volumes*, vol. 30, no. 6, pp. 23–33, 1997. IFAC Conference on Control of Industrial Systems ”Control for the Future of the Youth”, Belfort, France, 20-22 May.

[27] W. A. Saheri, N. A. A. Shashoa, and A. J. Abougarair, “Recursive least squares algorithm for miso carama systems utilizing data filtering,” in *2021 IEEE 1st International Maghreb Meeting of the Conference on Sciences and Techniques of Automatic Control and Computer Engineering MI-STA*, pp. 30–35, 2021.

[28] W. Sethares, C. Johnson, and C. Rohrs, “Bursting discovered in adaptive signal processing: Feedback to blame,” *IFAC Proceedings Volumes*, vol. 21, no. 10, pp. 27–32, 1988. IFAC Workshop on Robust Adaptive Control, Newcastle, Australia, 22-24 August.

[29] B. D. O. Anderson, “Failures of Adaptive Control Theory and their Resolution,” *Communications in Information Systems*, vol. 5, no. 1, pp. 1 – 20, 2005.

[30] B. D. Anderson and A. Dehghani, “Challenges of adaptive control–past, permanent and future,” *Annual Reviews in Control*, vol. 32, no. 2, pp. 123–135, 2008.

[31] D. Zhang, Z. Man, H. Wang, J. Zheng, Z. Cao, and S. Wang, “Online parameter estimation of linear systems using a new designed extended state observer,” in *2022 International Conference on Advanced Mechatronic Systems (ICAMechS)*, pp. 81–85, 2022.

[32] D. Zhang, Z. Man, H. Wang, J. Zheng, Z. Cao, and S. Wang, "A new extended sliding mode observer for second-order linear systems," in *2021 International Conference on Advanced Mechatronic Systems (ICAMechS)*, pp. 231–235, 2021.